Vibrational Transition Moments of Aminopurines: Stretched Film IR Linear Dichroism Measurements and DFT Calculations

Anders Holmén[†]

Department of Physical Chemistry, Chalmers University of Technology, S-412 96 Göteborg, Sweden

Received: January 31, 1997; In Final Form: April 8, 1997[⊗]

Vibrational transition moment directions for 7-methyladenine (7MA), 9-methyladenine (9MA), and 2-amino-9-methylpurine (2A9MP) have been determined from infrared linear dichroism measurements on samples partially oriented in stretched poly(vinyl alcohol) (PVA) films. The sign ambiguity problem for the experimental directions of 9MA and 2A9MP was in part solved by exploiting the change in orientation character of the ribose derivatives adenosine and 2-aminopurine riboside. In the case of all transitions in 7MA and most transitions in 9MA and 2A9MP, polarizations calculated in self-consistent-reaction-field (SCRF) DFT(B3LYP)/6-31G(d,p) calculations were used to guide the choice of experimental polarizations. The SCRF spectra were generally in better agreement with experiment than the corresponding calculated gas-phase spectra. The IR spectrum of adenine in PVA film was analyzed in terms of contributions from the 7-H and 9-H tautomers, and the relative abundance of the minor 7-H tautomer in PVA film was determined to be 23 ± 3% at room temperature.

Introduction

In order to interpret the vibrational circular dichroism (VCD)[1−3] and the infrared (IR) linear dichroism (LD)[4] spectra of nucleic acids, knowledge of the directions of the electric transition dipole moments of the vibrational transitions (IR transition moments) is crucial. Despite this fact, only a few attempts have been made to determine the the IR transition moment directions of the nucleic acid bases. Kyugoku *et al.* investigated the polarized IR spectra of single crystals of 1-methylthymine (1MT), 9-methyladenine (9MA), and the 1:1 complex of 1MT and 9MA.[5] This led to the identification of several in-plane- and out-of-plane-polarized transitions. Recently, in an investigation of the IR transition moments for 1,3-dimethyluracil, we found the carbonyl groups to be strongly coupled, leading to almost pure in-phase and out-of-phase carbonyl stretching vibrations.[6] The experimental IR polarizations were compared with those calculated at the HF/6-31G(d) level, and for most transitions, the calculated polarizations agreed within ±30° with one of the two possible experimental polarizations.

We here report on a combined experimental and quantum-chemical investigation of the IR transition moments of the purine base adenine, more specifically 9-methyladenine (9MA) and two of its structural isomers: 7-methyladenine (7MA) and 2-amino-9-methylpurine (2A9MP) (Figure 1). As a model of the adenine moiety found in nucleic acids, 9MA is a natural choice since the methyl group is at the same position as that of the sugar to which the adenine base is attached in nucleic acids. While the vibrational spectrum of the 9MA molecule has been studied extensively in various contexts,[7−11] the vibrational spectra of the structurally related chromophores 2A9MP and 7MA have, to the best of our knowledge, never been investigated.

In order to obtain the IR transition moments within the molecular framework, the mode of orientation in the stretched polymer film has to be characterized in terms of orientation parameters and direction of orientation axes. Such information is not only important for the determination of IR transition moments but also for the interpretation of UV LD measurements on these molecules in the same anisotropic hosts.[12,13] In previous UV LD studies on 9-substituted adenine derivatives in stretched films, lack of detailed knowledge of the orientational properties made it impossible to obtain more than relatively crude estimates of the electronic moment directions.[14−16]

For adenine and purine, NMR and UV measurements have shown that prototropic tautomerism in the imidazole ring exists in polar solvents.[17−19] This is expected to strongly influence spectroscopic measurements of adenine in PVA film and thus should previous UV LD measurements on adenine[16] be re-interpreted in terms of contributions from the 7-H and 9-H tautomers.[13] Therefore, we have investigated the IR spectra of the free bases in PVA film in order to clarify the tautomeric distribution in PVA film. The polarized IR spectra of 9MA and 2A9MP have been correlated with the spectra of the 9-substituted sugar derivatives adenosine and 2-aminopurine riboside in the search for vibrations that are characteristic of the 9-substituted adenine and 2-aminopurine chromophores.

The predictive capability of *ab initio* methods regarding IR transition moment directions has been evaluted by Radziszewski and co-workers for some small, low-symmetry, organic molecules, including ethylene-d_1,[20] propene,[21] and *s-trans*-1,3-butadiene.[22] These studies have shown that correct predictions of IR polarizations are difficult to make and that the convergence of the theoretical results is slow when going toward more sophisticated computatitional methods and that it is necessary to include some of the electron correlation in order to get reliable results. In this work, the assignment of the vibrational spectra and IR polarizations is aided by density-functional-theory (DFT) calculations using the recently developed B3LYP functional[23−25] with the 6-31G(d,p) basis set. Used in combination, these functional and basis set have been recently found to yield geometries, charge distributions, and vibrational spectra of heterocyclic molecules that are in good agreement with experimental data and with MP2 calculations.[26−31] In the case of 9MA, we have also performed MP2/6-31G(d) calculations to compare these data with those of the DFT method. In an attempt to model the effects of a polar solvent on the tautomeric

[†] Tel, +46 31 7723049; Fax, +46 31 7723858; E-mail, holmen@phc.chalmers.se.

[⊗] Abstract published in *Advance ACS Abstracts,* May 15, 1997.

S1089-5639(97)00381-2 CCC: $14.00

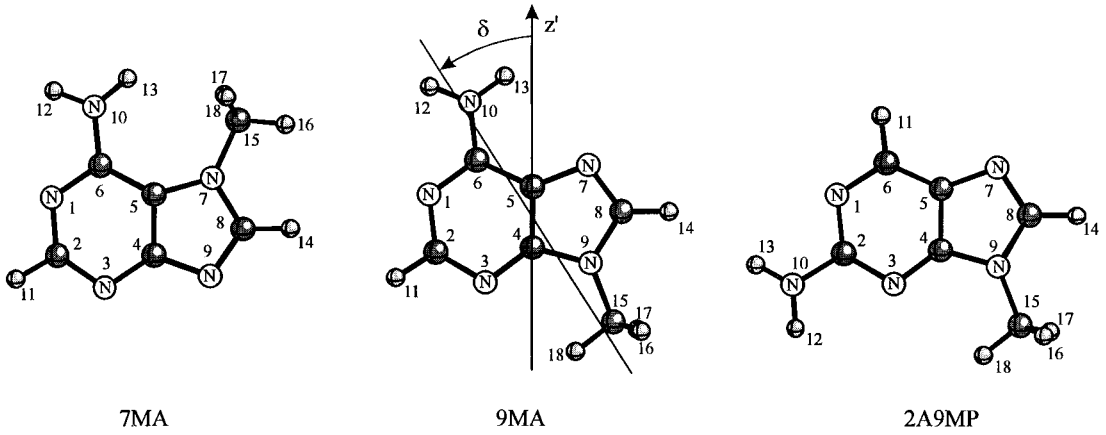

Figure 1. 7-methyladenine (7MA), 9-methyladenine (9MA), and 2-amino-9-methylpurine (2A9MP) molecules with atomic numbering and definition of an in-plane angle δ.

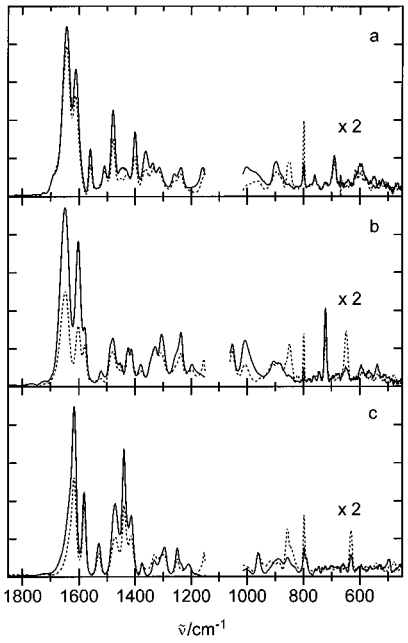

Figure 2. Polarized IR spectra, $A_{\parallel}$ (—) and $A_{\perp}$ (– –), of (a) 7MA, (b) 9MA, and (c) 2A9MP in stretched poly(vinyl alcohol) films.

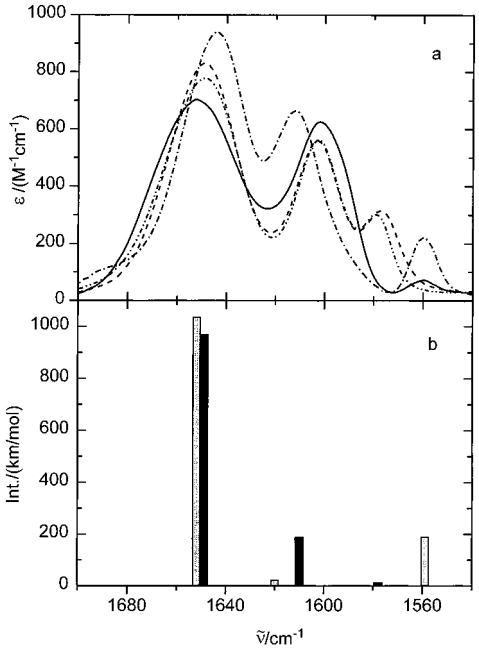

Figure 3. (a) Isotropic spectra of adenine (—), 7MA (—◇—), 9MA (—◇◇—) and Ado (– –) in PVA film in the 1700−1540 cm^{-1} region. (b) SCRF DFT(B3LYP)/6-31G(d,p)-calculated transitions of the 7-H (shaded bars) and 9-H (black bars) tautomers of adenine. The calculated frequencies have been scaled with the scaling factors obtained for 7MA and 9MA.[65]

equilibria and the vibrational spectra, the molecular geometries and IR spectra have been calculated in self-consistent-reaction-field (SCRF) calculations at the DFT(B3LYP)/6-31G(d,p) level, using the Onsager reaction-field model with a spherical cavity. The SCRF and gas-phase geometries of 7MA are found to be significantly different, which can be regarded as a consequence of the large dipole moment ($\mu_{vac} \approx 7$ D) of 7MA leading to a large solvent stabilization, which effects the predicted geometry. The SCRF IR spectrum and polarizations of 7MA are found to be in considerably better agreement with experimental solution (aqueous PVA matrix) data than the data obtained from the gas-phase calculation.

Materials and Experimental Methods

Chemicals. 2-aminopurine (2AP), 2-aminopurine riboside (2APr), adenine (A), and adenosine (Ado) were purchased from Sigma Chemical Co. and used without further purification. 2-amino-9-methylpurine (2A9MP) and 9-methyladenine were synthesized from 2-aminopurine and adenine, respectively, according to the methods described by Hedayatullah[32] and purified by chromatography on silica gel with chloroform/methanol/ammonia (45/15/1) as eluant and by subsequent recrystallization from ethanol/water. 7-methyladenine (7MA) was synthesized according to the methods described by Platzek *et al.*[33] and Denayer[34] and purified by chromatography on silica gel with chloroform/methanol/ammonia (45/15/1) as eluant and by subsequent crystallization from ethanol/water with charcoal. Deuterations in the eighth position and on the amino group were performed by repeated recrystallization of samples in boiling D_2O (Dr. Glaser AG., Basel). 9MA-*8-d* was obtained by dissolving 9MA-*8,12,13*-d_3 in H_2O at room temperature, where the amino hydrogens exchanged with the solvent. Poly(vinyl alcohol) (PVA) was obtained as a powder from E. I. du Pont de Nemours Co. All aqueous solutions were prepared with deionized water (Millipore). PVA films have been prepared as described before.[6] The molar absorptivities given in Figures 3a and 4a are based on the assumption that the molar absorptivity at 1580 cm^{-1} of adenosine in PVA film is the same as that of deoxyadenosine-5′-monophosphate in D_2O (ϵ(1580 cm^{-1}) = 300 cm^{-1} M^{-1}).[2] The concentration of the molecules in the stretched films was $\approx$ 0.1 M. At this concentration there were no signs of aggregation of the sample molecules.

IR Dichroism. Polarized IR measurements were performed on a Perkin-Elmer 1800 Fourier transform spectrometer. To obtain polarized IR radiation, a KRS-5 polarizer (IGP225

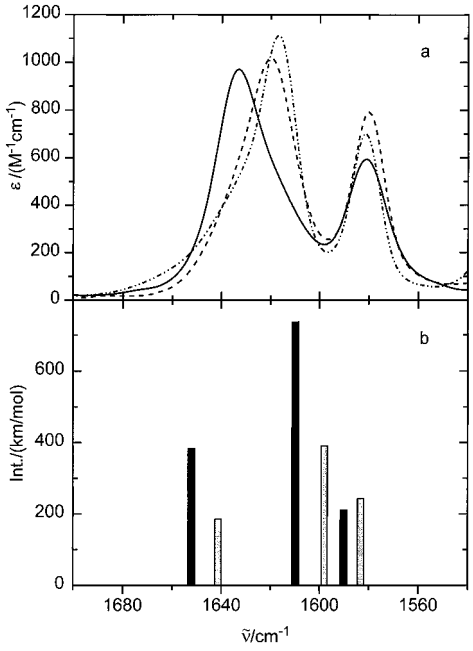

Figure 4. (a) Isotropic spectra of 2AP (—), 2A9MP (—◇◇—) and 2APr (— —) in PVA film in the 1700−1540 cm^{-1} region. (b) SCRF DFT(B3LYP)/6-31G(d,p) calculated transitions of the 7-H (shaded bars) and 9-H (black bars) tautomers of 2AP. The calculated frequencies have been scaled with a single scaling factor equal to 0.984.

Cambridge Physical Science) was placed in front of the sample. The spectral resolution was 2 cm^{-1} and each spectrum an average of 300 scans. A base line for PVA was recorded similarly and subtracted on an on line computer. IR spectra of polycrystalline samples in KBr tablets were also measured for reference.

The reduced linear dichroism, $LD^r(\tilde{\nu})$, was calculated according to[35,36]

$$LD^r(\tilde{\nu}) = 3(A_{\parallel}(\tilde{\nu}) - A_{\perp}(\tilde{\nu}))/(A_{\parallel}(\tilde{\nu}) + 2A_{\perp}(\tilde{\nu})) \quad (1)$$

where $A_{\parallel}(\tilde{\nu})$ and $A_{\perp}(\tilde{\nu})$ are the absorbances measured with plane polarized light, respectively, parallel and perpendicular to the stretching direction. For a planar molecule the LD^r for a pure in-plane-polarized transition i is related to the angle θ_i between the transition moment and the preferred molecular orientation axis z according to[16]

$$LD_i^r = 3(S_{yy} \sin^2 \theta_i + S_{zz} \cos^2 \theta_i) \quad (2)$$

where S_{yy} and S_{zz} are the Saupe orientation parameters[37] for the diagonal in-plane axes y and z. For a pure out-of-plane-polarized transition the LD_i^r is

$$LD_i^r = 3S_{xx} \quad (3)$$

The orientation parameters are interrelated according to[35]

$$3S_{yy} \le LD^r(\text{in-plane}) \le 3S_{zz} \quad (4)$$

$$S_{xx} + S_{yy} + S_{zz} = 0 \quad (5)$$

For overlapping transitions the intrinsic LD_i^r values were obtained by the TEM method developed by Thulstrup, Eggers, and Michl.[38] Given the orientation parameters, the polarizations of the in-plane IR transition moments relative to the molecular orientation axis were calculated using eq 2. The angle θ_i is related to the angle δ_i within the molecular framework and to the angle α that specifies the direction of the orientation axis by

$$\delta_i = \alpha \pm |\theta_i| \quad (6)$$

where δ_i and α are the angles between the z' axis (Figure 1) and the transition dipole moment direction and the orientation axis, respectively.

Symmetry of the Molecules. Strictly speaking, all molecules studied in this work are nonplanar and, thus, devoid of any symmetry (point group C_1). This means that there are no unique diagonal axes in the molecular coordinate system along which vibrations should be polarized. However, the major deviation from C_s symmetry for the methylated aminopurines (and also for adenine and 2AP) is due to the pyramidalization of the exocyclic amino group and, as judged from calculated moment of inertia for these molecules, the deviation from an "effective" C_s symmetry is very small (<2°). For the methylpurine fragment we thus expect 28 a′ and 14 a″ vibrations. The amino group gives rise to six additional vibrations, namely one symmetric and one antisymmetric stretching, one scissoring, one rocking, one twisting, and one wagging vibration of the amino group. The local C_1 symmetry of the amino group implies that none of these vibrations is expected to have either pure in-plane or pure out-of-plane polarization, although the deviations are expected to be small for the antisymmetric stretching (in-plane), rocking (in-plane), and inversion (out-of-plane) vibrations.[39] The assumption that the methylated aminopurines can be treated as planar molecules permits us to define the Saupe orientation parameters[37] related to a symmetry plane. These can therefore be determined as outlined in the Results section, in analogy with previous studies of near C_s-symmetric molecules like indole,[40] 7-methylpurine and 9-methylpurine,[41] 1,3-dimethyluracil,[6] and ϵ-adenine.[42] For the two molecules with ribose sugar moieties attached in the ninth position, Ado and 2APr, the deviation from an "effective" C_s symmetry is expected to be larger than for the methyl derivatives. However, we will again attempt the assumption that they behave as planar molecules and determine approximate orientation parameters for these molecules too.

Computational Methods

All quantum-chemical calculations were made with the Gaussian 94[43] (G94) package running on IBM RS6000-590 or Silicon Graphics INDY computers. Geometries were optimized for 7MA, 9MA, 2A9MP, and the 7-H and 9-H tautomers of adenine and 2AP using density functional theory (DFT) with the Becke three parameter hybrid functional (B3) for the exchange,[23] and the functional of Lee, Yang, and Parr[24] (LYP) for the correlation part. This method will hereafter be denoted DFT(B3LYP). The split valence standard 6-31G(d,p) basis set[44] was used in all DFT calculations. Additional calculations using second-order Møller−Plesset (MP2) perturbation theory,[45] with the 6-31G(d) basis set, were performed for 9MA. The effect of a polar solvent (water) was simulated in self-consistent-reaction-field (SCRF) optimizations at the DFT(B3LYP)/6-31G(d,p) level using the Onsager model with a spherical cavity.[46,47] For the prototropic tautomers of A and 2AP and for the aminomethylpurines, the radii 3.77 and 3.89 Å were used, respectively. The radii were determined according to the mass density approach developed by Karelson and Zerner.[48] Harmonic vibrational spectra were calculated for all optimized geometries at the corresponding levels of theory. The IR transition dipole moment directions were calculated from the dipole moment derivatives.

For the adenine and 2AP tautomers, thermal corrections to enthalpies and free energies at 298.15 K were calculated at the SCRF DFT(B3LYP)/6-31G(d,p) level with a single scaling factor of 0.96 for the vibrational frequencies using standard

TABLE 1: Definition of Internal Coordinates for 9MA, 7MA, and 2A9MP

coordinates[a]	description[b]
$S_1 = r_{1,2}$	νN_1C_2
$S_2 = r_{2,3}$	νC_2N_3
$S_3 = r_{3,4}$	νN_3C_4
$S_4 = r_{4,5}$	νC_4C_5
$S_5 = r_{5,6}$	νC_5C_6
$S_6 = r_{1,6}$	νN_1C_6
$S_7 = r_{5,7}$	νC_5N_7
$S_8 = r_{7,8}$	νN_7C_8
$S_9 = r_{8,9}$	νC_8N_9
$S_{10} = r_{4,9}$	νC_4N_9
$S_{11} = r_{2,11}$	νC_2H_{11}[c]
$S_{12} = r_{6,10}$	νC_6N_{10}[d]
$S_{13} = r_{8,14}$	νC_8H_{14}
$S_{14} = r_{9,15}$	νN_9C_{15}[e]
$S_{15} = 2^{-1/2}(\beta_{1,2,11} - \beta_{3,2,11})$	δC_2H_{11}[f]
$S_{16} = 2^{-1/2}(\beta_{1,6,10} - \beta_{5,6,10})$	δC_6N_{10}[g]
$S_{17} = 2^{-1/2}(\beta_{7,8,14} - \beta_{9,8,14})$	δC_8H_{14}
$S_{18} = 2^{-1/2}(\beta_{4,9,15} - \beta_{8,9,15})$	δN_9C_{15}[h]
$S_{19} = \gamma_{11,2,3,1}$	γC_2H_{11}[i]
$S_{20} = \gamma_{10,6,1,5}$	γC_6N_{10}[j]
$S_{21} = \gamma_{14,8,7,9}$	γC_8H_{14}
$S_{22} = \gamma_{15,9,4,8}$	γN_9C_{15}[k]
$S_{23} = 6^{-1/2}(\beta_{1,2,6} - \beta_{1,2,3} + \beta_{2,3,4} - \beta_{3,4,5} + \beta_{4,5,6} - \beta_{5,6,1})$	δ(6-ring 1)
$S_{24} = 12^{-1/2}(2\beta_{1,2,6} - \beta_{1,2,3} - \beta_{2,3,4} + 2\beta_{3,4,5} - \beta_{4,5,6} - \beta_{5,6,1})$	δ(6-ring 2)
$S_{25} = 1/2(\beta_{1,2,3} - \beta_{2,3,4} + \beta_{4,5,6} - \beta_{5,6,1})$	δ(6-ring 3)
$S_{26} = 6^{-1/2}(\tau_{1,2,3,4} - \tau_{2,3,4,5} + \tau_{3,4,5,6} - \tau_{4,5,6,1} + \tau_{5,6,1,2} - \tau_{6,1,2,3})$	τ(6-ring 1)
$S_{27} = 1/2(\tau_{1,2,3,4} - \tau_{3,4,5,6} + \tau_{4,5,6,1} - \tau_{6,1,2,3})$	τ(6-ring 2)
$S_{28} = 12^{-1/2}(-\tau_{1,2,3,4} + 2\tau_{2,3,4,5} - \tau_{3,4,5,6} - \tau_{4,5,6,1} + 2\tau_{5,6,1,2} - \tau_{6,1,2,3})$	τ(6-ring 3)
$S_{29} = (1 + 2a^2 + 2b^2)^{-1/2}[\beta_{4,8,9} + a(\beta_{5,4,9} + \beta_{7,9,8}) + b(\beta_{4,5,7} + \beta_{5,7,8})]$	δ(5-ring 1)
$S_{30} = [2(a - b)^2 + 2(1 - a)^2]^{-1/2}[(a - b)(\beta_{5,4,9} - \beta_{7,9,8}) - (1 - a)(\beta_{4,5,7} - \beta_{5,7,8})]$	δ(5-ring 2)
$S_{31} = (1 + 2a^2 + 2b^2)^{-1/2}[(\tau_{4,5,7,8} + a(\tau_{9,4,5,7} + \tau_{5,7,8,9}) + b(\tau_{8,9,4,5} + \tau_{7,8,9,4})]$	τ(5-ring 1)
$S_{32} = [2(a - b)^2 + 2(1 - a)^2]^{-1/2}[(a - b)(\tau_{5,7,8,9} - \tau_{9,4,5,7}) - (1 - a)(\tau_{7,8,9,4} - \tau_{8,9,4,5})]$	τ(5-ring 2)
$S_{33} = 2^{-1/2}(\tau_{6,5,4,9} - \tau_{3,4,5,7})$	τ(5/6 ring)
$S_{34} = 2^{-1/2}(r_{10,12} + r_{10,12})$	ν_sNH_2
$S_{35} = 2^{-1/2}(r_{10,12} - r_{10,13})$	$\nu_{as}NH_2$
$S_{36} = 6^{-1/2}(2\beta_{12,10,13} - \beta_{6,10,12} - \beta_{6,10,13})$[l]	δ_sNH_2 (soring)
$S_{37} = 2^{-1/2}(\beta_{6,10,13} - \beta_{6,10,12})$[l]	$\delta_{as}NH_2$ (rock)
$S_{38} = 1/2(\tau_{1,6,10,12} + \tau_{1,6,10,13} + \tau_{5,6,10,12} + \tau_{5,6,10,12})$[m]	τNH_2 (torsional)
$S_{39} = \gamma_{6,10,12,13}$[n]	γNH_2 (wagging)
$S_{40} = 3^{-1/2}(r_{15,16} + r_{15,17} + r_{15,18})$	ν_sCH_3
$S_{41} = 6^{-1/2}(2r_{15,16} - r_{15,17} - r_{15,18})$	$\nu_{as}CH_3$
$S_{42} = 2^{-1/2}(r_{15,18} - r_{15,17})$	$\nu_{as}CH_3$ (out-of-plane)
$S_{43} = 6^{-1/2}(\beta_{16,15,17} + \beta_{16,15,18} + \beta_{17,15,18} - \beta_{9,15,16} - \beta_{9,15,17} - \beta_{9,15,18})$[o]	δ_sCH_3
$S_{44} = 6^{-1/2}(2\beta_{17,15,18} - \beta_{16,15,17} - \beta_{16,15,18})$	$\delta_{as}CH_3$
$S_{45} = 6^{-1/2}(2\beta_{9,15,16} - \beta_{9,15,17} - \beta_{9,15,18})$[o]	$\delta_{as}CH_3$
$S_{46} = 2^{-1/2}(\beta_{16,15,18} - \beta_{16,15,17})$	$\delta_{as}CH_3$ (out-of-plane)
$S_{47} = 2^{-1/2}(\beta_{9,15,18} - \beta_{9,15,17})$[o]	$\delta_{as}CH_3$ (out-of-plane)
$S_{48} = 3^{-1/2}(\tau_{8,9,15,16} + \tau_{8,9,15,17} + \tau_{8,9,15,18})$[p]	τCH_3

[a] $r_{i,j}$ = the bond distance between atoms i and j; $\beta_{i,j,k}$ = the bond angle involving atoms i, j, and k; $\gamma_{i,j,k,l}$ = the out-of-plane angle between the vector i, j and the j, k, l plane; $\tau_{i,j,k,l}$ = the torsion angle involving atoms i, j, k, and l; $a = \cos 144° = -0.8090$ and $b = \cos 72° = 0.3090$. [b] ν, ν_s, ν_{as}, δ, δ_s, δ_{as}, γ, τ, and ρ denote in-plane stretching, symmetric stretching, asymmetric stretching, in-plane bending, symmetric bending, asymmetric bending, out-of-plane bending, and torsion and rocking, respectively. The use of the descriptions in-plane and out-of-plane refer to the pseudo-C_s-symmetry plane comprising the purine ring system. [c] C_2N_{10} for 2A9MP. [d] C_6H_{11} for 2A9MP. [e] $r_{7,15}$ and νN_7C_{15} for 7MA. [f] $\beta_{1,2,10} - \beta_{3,2,10}$ and δC_2N_{10} for 2A9MP. [g] $\beta_{1,6,11} - \beta_{5,6,11}$ and δC_6H_{11} for 2A9MP. [h] $\beta_{5,7,15} - \beta_{8,7,15}$ and δN_7C_{15} for 7MA. [i] $\gamma_{10,2,3,1}$ and γC_2N_{10} for 2A9MP. [j] $\gamma_{11,6,1,5}$ and γC_6H_{11} for 2A9MP. [k] $\gamma_{15,7,5,8}$ and γN_7C_{15} for 7MA. [l] $\beta_{12,10,13}$, $\beta_{2,10,12}$ and $\beta_{2,10,13}$ for 2A9MP. [m] $\tau_{1,2,10,12}$, $\tau_{1,2,10,13}$, $\tau_{3,2,10,12}$, and $\tau_{3,2,10,13}$ for 2A9MP. [n] $\gamma_{2,10,12,13}$ for 2A9MP. [o] $\beta_{7,15,16}$, $\beta_{7,15,17}$, and $\beta_{7,15,18}$ for 7MA. [p] $\tau_{8,7,15,16}$, $\tau_{8,7,15,17}$, and $\tau_{8,7,15,18}$ for 7MA.

procedures in G94. In addition, single-point calculations at the SCRF geometries of the adenine and 2AP tautomers were performed with the polarized-continuum model (PCM) in order to simulate water solution.[49,50] The $\Delta G = G_{7-\mathrm{Htaut}} - G_{9-\mathrm{Htaut}}$ for the 9-H/7-H tautomeric equilibrium (see Discussion) at 298.15 K was estimated as

$$\Delta G(298\ \mathrm{K}) = \Delta G(\mathrm{solv,PCM}) + \Delta E(0\ \mathrm{K,gas\text{-}phase}) + \Delta(\mathrm{G(SCRF_{corr})}) \quad (7)$$

where ΔG(solv,PCM) is the difference between the solvation energies for the 7-H and 9-H tautomers obtained in the PCM calculation, ΔE(0 K,gas-phase) is the difference in internal energies at 0 K obtained at the gas-phase geometries and Δ(G(SCRF$_{corr}$)) is the difference in thermochemical correction to free energies at 298.15 K calculated in the SCRF calculations, including the difference in zero-point energies. For a description of the different components contributing to the PCM solvation energy see Coitiño and Tomasi.[51] The atomic radii used in the PCM calculation were those belonging to the so-called Pauling's set reported by Cossi *et al.*[50] The PCM routine was kindly provided by Professor Jacopo Tomasi, Pisa.

Normal coordinate analyses (NCA) were performed with the program INTDER95.[52,53] The internal coordinates used in the NCA are given in Table 1. The total energy distribution (TED) were calculated according to Allen *et al.*[54]

Results

IR Linear Dichroism. The polarized IR spectra ($A_{\|}$ and $A_{\perp}$) of 7MA, 9MA, and 2A9MP in stretched PVA films are shown

TABLE 2: Observed Vibrational Transitions of 7MA, 9MA, 9MA-*8-d* and 2A9MP in PVA Film, Their LD^r and Polarization

7MA			9MA			9MA-*8-d*			2A9MP		
$\tilde{\nu}$/cm^{-1}	LD^r	$\|\theta\|^a$	$\tilde{\nu}$/cm^{-1}	LD^r	$\|\theta\|^a$	$\tilde{\nu}$/cm^{-1}	LD^r	$\|\theta\|^a$	$\tilde{\nu}$/cm^{-1}	LD^r	$\|\theta\|^a$
1644 (vs)	0.15	84 ± 6	1649 (vs)	0.75	28	1649 (vs)	0.74	29	1640 (sh)	0.66	18 ± 3
1612 (s)	0.38	50 ± 1	1603 (s)	**0.95**[b]	0	1601 (s)	**0.95**[b]	0	1617 (s)	0.64	24 ± 3
1560 (m)	0.41	47 ± 1	1577 (m)	0.12	72	1577 (m)	0.12	72	1582 (s)	0.20	67 ± 2
1510 (w)	0.32	56 ± 1	1522 (vw)	0.73	30	1506 (vw)	0.31	57	1529 (m)	0.34	52 ± 2
			1487 (sh)	0.30	57	1487 (sh)	0.65	35			
1479 (m)	0.43	45 ± 1	1477 (m)	0.30	57	1477 (m)	0.67	34	1470 (m)	0.70	15 ± 5
1450 (vw)	0.59	29 ± 1	1434 (sh)	0.43	49						
1429 (vw)	0.17	76 ± 3	1425 (w)	**0.03**	90	1418 (sh)	**0.03**	0	1439 (s)	0.61	27 ± 3
1401 (m)	0.61	26 ± 1	1413 (w)	**0.03**	90	1401 (m)	0.15	69	1414 (m)	0.49	38 ± 2
1370 (sh)	0.51	37 ± 1	1380 (w)	0.90	15	1378 (w)	0.91	13	1375 (w)	0.55	33 ± 2
1362 (w)	0.72	6 ± 6	1345 (sh)	0.07	78	1340 (sh)	**0.03**	90	1332 (w)	0.11	85 ± 5
1337 (w)	0.37	51 ± 1	1328 (m)	0.04	84	1320 (m)	0.20	65	1309 (sh)	0.73	8 ± 8
1314 (w)	0.15	84 ± 6	1305 (m)	0.94	8	1305 (m)	0.94	8	1294 (w)	0.59	27 ± 3
1260 (vw)	0.42	46 ± 1	1255 (sh)	0.91	13	1257 (w)	0.93	10	1250 (w)	0.46	41 ± 2
1237 (vw)	0.38	50 ± 1	1236 (m)	0.62	37				1208 (w)	0.20	67 ± 2
1159 (vw)	0.29	59 ± 1	1196 (vw)	0.32	56						
1070	ND[c]		1053 (vw)	0.04	84	1069 (vw)	**0.03**	90	1047	ND[c]	
1001	ND[c]		1007 (vw)	0.53	43	1008 (vw)	0.74	29	963 (w)	0.28	58 ± 2
			954 (vw)	**−0.96**	oop[d]						
						938 (w)	0.51	44			
									915 (vw)	**−0.84**[b]	oop
897 (vw)	0.66	20 ± 2	905(vw)	0.21	64	878 (vw)	0.67	34	889 (vw)	0.14	77 ± 3
875 (sh)	**−0.85**[b]	oop	837 (vw)	**−1.00**	oop	819 (vw)			855 (vw)	**−0.84**	oop
799 (w)	**−0.88**	oop	798 (w)	**−0.98**	oop	799 (m)	**−0.98**	oop	797 (w)	**−0.81**	oop
760 (vw)	0.39	49 ± 1	745 (w)	0.51	44	741 (vw)	0.38	52	789 (vw)	0.34	52 ± 2
690 (vw)	0.35	53 ± 1	721 (m)	0.65	35	714 (m)	0.74	29			
			648 (w)	**−1.00**	oop	645 (vw)	**−0.98**	oop			
						600 (w)	**−0.98**	oop	631 (w)	**−0.86**	oop
			595 (vw)	0.75	28						
			537 (vw)	0.67	34	536 (vw)	0.52	43			
			479 (vw)	**−1.00**	oop	479 (vw)	**−1.00**	oop			

[a] Transition moment direction in degrees relative the orientation axis. Uncertainties for 7MA and 2A9MP estimated from the uncertainities in the orientation parameters. [b] Boldface numbers denote LD^r values that have been used to estimate the orientation parameters. [c] ND = not determined due to too high PVA absorption in the perpendicular component. [d] oop = out-of-plane vibration.

in Figure 2. Since strong base line (PVA) absorption occurs below 450 cm $^{-1}$ and in the 3500−2700 cm^{-1} region where NH and CH stretching vibrations are expected (*vide infra*), the spectral analysis is limited to the region between 1850 and 450 cm^{-1}. Furthermore, strong base line absorption in the perpendicular component ($A_\perp$) at about 1150−1050 cm^{-1}, prevents a reliable base line subtraction in this region, and, consequently, the determination of LD^r values for vibrations in this region. The data deduced from the TEM analysis of the polarized spectra are summarized in Table 2. One deuterated derivative of 9MA has also been examined in PVA film, namely 9MA-*8-d*, which is included in the study for two reasons. Firstly, both 9MA and 9MA-*8-d* are expected to have nearly identical orientation characteristics (orientation parameters and orientation axis) but to differ in several of the observed vibrations, thereby giving rise to two complementary sets of transitions which could increase the reliability in determined orientation parameters and in the assignment of an in-plane orientation axis for the 9MA chromophore. Secondly, the observed spectral shifts upon deuteration helps in the assignment of the vibrational transitions of 9MA. The isotropic IR spectra in the 1700−1540 cm^{-1} region of adenine, 7MA, 9MA, and Ado and 2AP, 2A9MP, and 2APr are displayed in Figures 3 and 4. In Table 1S (Supporting Information) the experimental data for Ado, 2APr, adenine, and 2AP are collected.

In order to calculate the angles between the moment directions and orientation axis, we need to determine the orientation parameters S_{xx}, S_{yy}, and S_{zz}. For 9MA and 9MA-*8-d*, the out-of-plane parameter S_{xx} is calculated from the average of the LD^r values for the out-of-plane-polarized transitions (eq 3). This is motivated by that eight out of nine observed LD^r values give the same value of S_{xx} within the experimental accuracy. This leads to $S_{xx} = -0.33$. The same approach is used for Ado, 2APr, A, and 2AP (Table 1S). In the case of 7MA the range of observed $S_{xx} = -0.28$ to -0.29, with an average of $S_{xx} = -0.29$. 2A9MP has a slightly broader interval of observed S_{xx} of -0.27 to -0.29, with an average of $S_{xx} = -0.28$.

TABLE 3: Observed Orientation Parameters in PVA Film and Chosen Directions of the Orientation Axis (OA) for 7MA, 9MA, 2A9MP, A, 2AP, Ado, and 2APr

compd	S_{zz}	S_{yy}	S_{xx}	α(OA)/deg
7MA	0.24	0.05	−0.29	-72 ± 5^a
9MA	0.32	0.01	−0.33	$+51 \pm 5^b$
2A9MP	0.24	0.04	−0.28	$+87 \pm 5^a$
7-H-A	0.29	0.01	−0.30	$+66^a$
9-H-A				$+67^a$
7-H-2AP	0.33	0.00	−0.33	-77^a
9-H-2AP				-76^a
Ado	0.26	0.01	−0.27	$\approx+45^b$
2APr	0.20	0.01	−0.21	$\approx+77^b$

[a] Direction of the minimum principal moment of inertia axis with respect to the z' axis (Figure 1). [b] See text for discussion.

In order to estimate the in-plane parameters S_{yy} and S_{zz}, an approximate method is used. We expect that at least one of the observed in-plane vibrations for each molecule is polarized either closely parallel or perpendicular to the orientation axis. The corresponding LD^r value of this transition, which is an in-plane extreme value, gives an approximate value of the appropriate orientation parameter. For all molecules studied, the observed minimum and maximum in-plane LD^r values correspond to orientation parameters that together with the average S_{xx} values obey the sum rule for the orientation parameters (eq 5) (Table 3). This indicates that the determined orientation parameters are probably quite reliable. If it is assumed that the entire uncertainty in the orientation parameters is determined by the uncertainty in the out-of-plane parameter

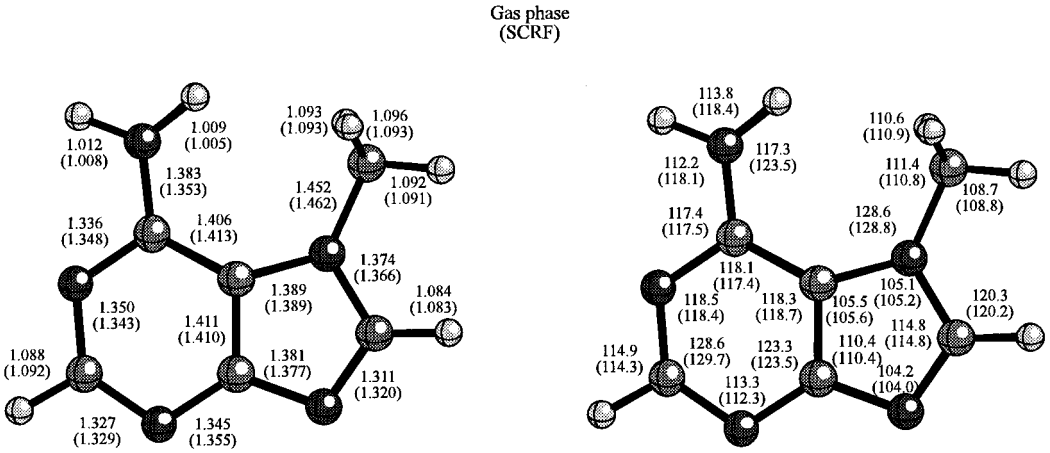

Dihedral angles:

N1-C2-N3-C4	-0.9 (0.0)	C4-N3-C2-H11	179.6 (180.0)
N1-C6-N10-H12	12.8 (0.1)	C4-N9-C8-H14	-179.7 (180.0)
C2-N3-C4-N9	-178.9 (180.0)	C4-C5-N7-C15	179.1 (180.0)
N3-C4-C5-C6	-1.0 (0.0)	C5-C6-N10-H13	-35.5 (-0.1)
N3-C4-C5-N7	-178.8 (180.0)	C5-N7-C15-H16	-171.1 (180.0)
N3-C4-N9-C8	178.9 (180.0)	C5-N7-C15-H17	-52.1 (-61.3)
C4-C5-C6-N10	-178.1 (180.0)	C5-N7-C15-H18	69.8 (61.2)

Figure 5. DFT(B3LYP)/6-31G(d,p) and SCRF DFT(B3LYP)/6-31G(d,p) geometries of 7MA

S_{xx}, then S_{zz} and S_{yy} of 7MA are in the intervals [0.24,0.25] and [0.04,0.05], respectively. For 2A9MP, we obtain S_{zz} = [0.24,0.26] and S_{yy} = [0.03,0.05]. The uncertainties in the orientation parameters introduce uncertainties in the final transition moment directions. The IR polarizations relative the orientation axes are given in Table 2 with error bars estimated from the uncertainties in the orientation parameters.

To obtain the absolute moment directions within the molecular coordinate system (*i.e.*, relative to the z' axis in Figure 1) we need to determine the direction of the orientation axis within the molecular coordinate system. Due to the absence of symmetry of the molecules, except for the approximate symmetry plane defined by the ring system, it is not straightforward to *a priori* assign an orientation axis direction. However, experience from previous studies has shown that in a uniaxial polymer medium, such as a film of polyethylene or poly(vinyl alcohol), the solute molecules tend to orient with their smallest cross section perpendicular to the stretching direction.[36,55] Thus, it is reasonable to assume that the orientation axis direction can be estimated as the axis of minimum principal moment of inertia which coincides approximately with the longest molecular dimension. The directions of the moment of inertia axes are taken from the SCRF DFT(B3LYP)/6-31G(d,p) geometry optimizations and are collected in Table 3. We will hereafter use these directions for 7MA and 2A9MP. In the case of 9MA and 9MA-*8-d*, the inertial axis was used as a first trial of the orientation axis in a least-squares fit between experimental and calculated polarizations to obtain the best choice of orientation axis. A total of 32 in-plane vibrations were used in the fit. Vibrations that were calculated to have methyl group deformation character were not included in the fit due to their often mixed in-plane and out-of-plane polarizations. A +2° rotation from the first assumed (moment of inertia) orientation axis direction, +49° (Table 3), gave the best overall fit. The directions of the orientation axes of 7MA, 9MA, and 2A9MP are estimated to be correct within ±5° from experience of molecules with similar shape.[40,41]

Quantum Chemical Calculations. The geometries of 7MA, 9MA and 2A9MP, optimized at the DFT(B3LYP)/6-31G(d,p) and SCRF DFT(B3LYP)/6-31G(d,p) levels, are shown in Figures 5, 6, and 7, respectively. The calculated IR spectra at the SCRF DFT(B3LYP)/6-31G(d,p) level of 7MA, 9MA, and 2A9MP are presented in Tables 4, 5, and 6, respectively, together with the experimental data for samples in PVA film and in KBr tablets. The MP2/6-31G(d) IR spectrum of 9MA is presented in Table 2S, and the DFT(B3LYP)/6-31G(d,p) IR spectra of 7MA, 9MA, and 2A9MP are collected in Tables 3S, 4S, and 5S, respectively. The calculated spectra in the 1700−1540 cm^{-1} region the of the 7-H and 9-H tautomers of adenine and 2AP are displayed in Figures 3 and 4.

Discussion

Calculated Molecular Structures and Spectra. The DFT-(B3LYP)/6-31G(d,p) geometries of 7MA (Figure 5) and 9MA (Figure 6) are very similar to the MP2/6-31G(d) geometries reported by Holmén *et al.*,[56] and in the case of 9MA, the MP2 and the DFT(B3LYP) geometries and the neutron diffraction structure reported by Mcmullan *et al.*[57] were in both cases equal within 0.008 Å in bond lengths.[29] The DFT(B3LYP)/6-31G(d,p) and the MP2/6-31G(d) (Table 5S) IR spectra of 9MA, however, differ significantly for a few vibrations. One example is the ring torsion mode, found for all the studied purine derivatives between 797−800 cm^{-1}, which for 9MA was observed at 798 cm^{-1} in the PVA matrix and at 797 cm^{-1} in KBr pellet. This vibration was predicted to occur at 808 cm^{-1} and at 698 cm^{-1} in the DFT(B3LYP) and MP2 calculations, respectively. With only the MP2 calculation at hand it would have been natural to assign the vibration calculated at 815 cm^{-1} (Table 5S) to be the peak observed at 798 cm^{-1}. The 815 cm^{-1} transition is the γC_8H mode which experimentally, due to comparison with 9MA-*8-d*, is assigned with confidence to the observed transition at 843 cm^{-1} in KBr tablet and calculated by DFT(B3LYP) theory to be at 865 cm^{-1}. Thus, it seems that in the case of 9MA, the DFT-based methods perform better than the MP2 method in the sense that we have not found any contradictions between the DFT calculated order and character of the vibrations and those assignments which are based solely on experimental data.

In the series of methylated aminopurines, the calculated gas-phase dipole moments vary between 2.45 D for 9MA, 3.68 D for 2A9MP, and up to 7.21 D for 7MA, and the corresponding SCRF (water) values are 3.82, 5.03, and 11.09 D, respectively.

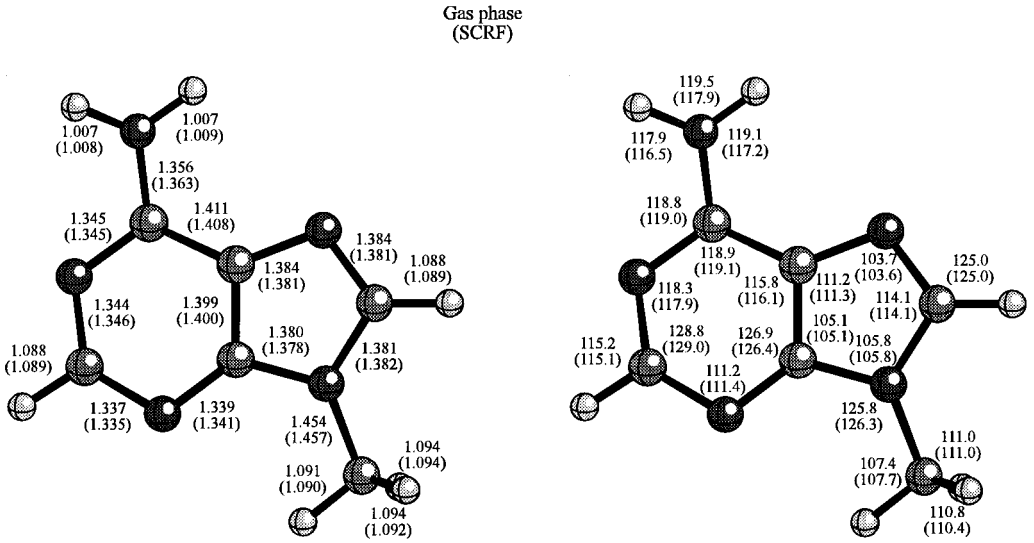

Dihedral angles:

N1-C2-N3-C4	0.1 (0.1)	C4-N3-C2-H11	-179.8 (-179.7)
N1-C6-N10-H12	10.9 (17.3)	C4-N9-C8-H14	179.9 (179.7)
C2-N3-C4-N9	179.5 (178.7)	C4-N9-C15-H16	-121.7 (-129.0)
N3-C4-C5-C6	0.0 (0.5)	C4-N9-C15-H17	116.8 (109.7)
N3-C4-C5-N7	179.6 (179.3)	C4-N9-C15-H18	-2.5 (-9.7)
N3-C4-N9-C8	-179.6 (-179.3)	C5-C4-N9-C15	-179.7 (-179.8)
C4-C5-C6-N10	-178.6 (-178.7)	C5-C6-N10-H13	-11.8 (-16.3)

Figure 6. DFT(B3LYP)/6-31G(d,p) and SCRF DFT(B3LYP)/6-31G(d,p) geometries of 9MA.

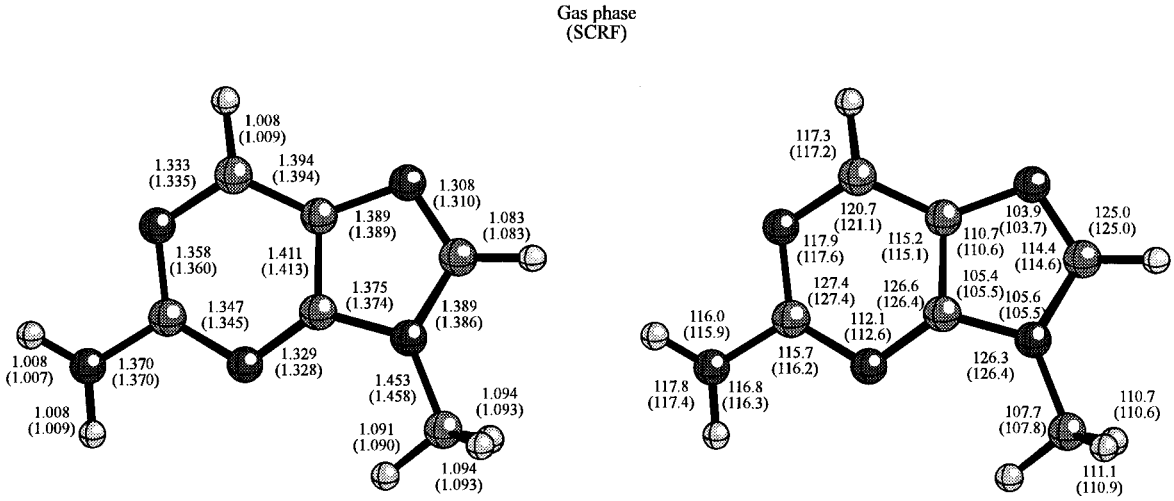

Dihedral angles:

N1-C2-N3-C4	-1.0 (-0.9)	C4-N3-C2-N10	177.5 (177.5)
N1-C2-N10-H13	-17.3 (-19.7)	C4-C5-C6-H11	179.3 (179.0)
C2-N3-C4-N9	-179.8 (179.8)	C4-N9-C15-H16	-114.2 (-113.7)
N3-C4-C5-C6	0.3 (0.6)	C4-N9-C15-H17	124.3 (124.9)
N3-C4-C5-N7	179.8 (179.8)	C4-N9-C15-H18	5.1 (5.6)
N3-C4-N9-C8	-179.8 (-179.3)	C4-N9-C8-H14	-179.9 (180.0)
N3-C2-N10-H12	18.2 (17.2)	C5-C4-N9-C15	-179.7 (-179.8)

Figure 7. DFT(B3LYP)/6-31G(d,p) and SCRF DFT(B3LYP)/6-31G(d,p) geometries of 2A9MP.

The increase of the dipole moments upon solvation in absolute terms, is the largest for 7MA ($\Delta\mu = 3.88$ D), while it is about the same for 9MA ($\Delta\mu = 1.37$ D) and 2A9MP ($\Delta\mu = 1.35$ D). The differences between the gas-phase and SCRF geometries and the vibrational spectra follow the same trend with relatively small changes for 9MA and 2A9MP and relatively large changes in the geometry and consequently in the vibrational spectrum of 7MA. Interesting to note is the effect on the amino group pyramidalization upon solvation. The hybridization of the amino group of 7MA becomes more sp^2 like as seen from the shorter C6−N10 bond and the nearly planar amino group, in contrast to the gas-phase geometry where the amino group hydrogens point unsymmetrically out of the plane. For 2A9MP, there is very little change while for 9MA the amino group shows more sp^3 character in the dielectric continuum approach. For 7MA, the overall agreement with the experimental solution phase (PVA) data is significantly better for the SCRF calculation compared to the gas-phase calculation, which indicates that for

TABLE 4: Comparison of Experimental and Calculated IR Spectra of 7-Methyladenine

	exptl[a]			calcd (SCRF DFT(B3LYP)/6-31G(d,p))				
mode	$\tilde{\nu}$(PVA)/ cm^{-1}	δ^b/ deg	$\tilde{\nu}$(KBr)/ cm^{-1}	$\tilde{\nu}$/ cm^{-1}	IR int/ (km/mol)	δ^c/ deg	TED[d]	assignt[e]
1			3325 (s)	3760	131	−73	$S_{35}(99)$	$\nu_{as}NH_2$
2			3151 (s)	3626	238	22	$S_{34}(98)$	$\nu_{s}NH_2$
3			3081 (w)	3247	1	−47	$S_{13}(99)$	νC_8H_{14}
4			3065 (vw)	3166	2	73	$S_{41}(96)$	$\nu_{as}CH_3$
			3048 (vw)					$\nu_{10} + \nu_{13} = 3038$
5			2985 (sh)	3137	6	oop[g]	$S_{42}(100)$	$\nu_{as}CH_3$
6			2976(w)	3117	201	−57	$S_{11}(100)$	νC_2H_{11}
			2958 (vw)					$\nu_{13} + \nu_{14} = 2950$
7			2914 (vvw)	3063	24	−21	$S_{40}(96)$	$\nu_{s}CH_3$
			2876 (vvw)					$\nu_{14} + \nu_{15} = 2889$
			2817 (vvw)					$\nu_{15} + \nu_{16} = 2821$
			2664 (vvw)					$\nu_{18} + \nu_{20} = 2671$
			2607 (vvw)					$2\nu_{20} = 2618$
			1814 (vvw)					$2\nu_{28} = 1818$
8	1644 (vs)	+24 ± 11	1666 (vs)	1666	1050	18	$S_{36}(41) + S_{12}(22) - S_5(18)$	$\delta_{s}NH_2$ (scissoring)
9	1612 (s)	+58 ± 6	1607 (vs)	1634	63	49	$S_{36}(37) + S_5(19) + S_2(8) - S_7(8)$	ν(ring), $\delta_{s}NH_2$ (scissoring)
10	1560 (m)	−25 ± 6	1552 (s)	1591	97	−22	$S_3(22) - S_4(13) + S_6(11) + S_{25}(9)$	ν(6-ring)
11	1510 (w)	−16 ± 6	1513 (vw)	1536	96	−30	$S_9(20) + S_{17}(12) + S_{15}(9) + S_3(8)$	ν(ring)
12				1529	66	76	$S_{44}(79) + S_{45}(11)$	$\delta_{as}CH_3$
13	1479 (m)	−27 ± 6	1486 (s)	1511	228	−35	$S_{15}(24) - S_6(20) + S_2(16) - S_{17}(9)$	ν(6-ring)
14	1450 (vw)	−44/80 ± 6	1464 (w)	1497	18	oop	$S_{46}(93) - S_{47}(8)$	$\delta_{as}CH_3$
15	1429 (vw)	32 ± 8	1425 (w)	1467	14	55	$S_{43}(76) + S_9(12)$	$\delta_{s}CH_3$
16	1401 (m)	−46 ± 6	1396 (m)	1424	194	−48	$S_{30}(17) + S_4(13) + S_{14}(11) + S_{43}(10)$	ν(5-ring)
17	1370 (sh)	−35 ± 6	1372 (w)	1405	12	−21	$S_9(25) - S_{12}(12) + S_{23}(11) + S_7(10)$	ν(5-ring)
18	1362 (w)	−78 ± 6	1362 (w)	1382	64	88	$S_1(19) - S_8(15) + S_7(11) + S_{15}(9)$	ν(ring)
19	1337 (w)	+57 ± 6	1343 (w)	1376	73	40	$S_{15}(35) - S_2(17) + S_8(12) + S_{45}(6)$	δC_2H_{11}
20	1314 (w)	24 ± 11	1309 (w)	1350	73	68	$S_{10}(23) - S_3(18) + S_6(17) - S_1(10)$	ν(ring)
21	1260 (vw)	−26 ± 6	1258 (w)	1297	20	−6	$S_1(26) + S_2(25) - S_{37}(10) - S_{16}(6)$	ν(6-ring)
22	1237 (vw)	−22 ± 6	1235 (w)	1267	95	−32	$S_{17}(57) - S_9(11) - S_{14}(8)$	δC_8H_{14}
23	1159 (vw)	49 ± 6	1165 (w)	1171	52	49	$S_{30}(19) + S_{37}(15) + S_{14}(10) + S_{10}(8)$	δ(5-ring)
24			1091 (vw)	1143	0.4	oop	$S_{47}(91) + S_{46}(8)$	$\delta_{as}CH_3$
25			1068 (vw)	1104	9	26	$S_{23}(14) + S_{45}(12) + S_{29}(10) - S_3(10)$	δ(ring)
26	1070	ND[f]	1052 (w)	1071	33	0	$S_{45}(43) - S_8(25) - S_{29}(15) + S_4(8)$	$\delta_{as}CH_3$
27	1001		1014 (w)	1001	15	44	$S_{37}(48) + S_6(31) + S_1(10) + S_{12}(4)$	$\delta_{as}NH_2$ (rock)
28			970 (vvw)	960	1	oop	$S_{19}(109) - S_{27}(-5) - S_{26}(-4)$	γC_2H_{11}
29	897 (vw)	−53 ± 5	909/891 (w)	900	35	−49	$S_{23}(52) - S_{29}(14) + S_{10}(7) + S_{24}(6)$	δ(6-ring)
30	875 (sh)	oop	879 (sh)	882	10	oop	$S_{21}(102) + S_{32}(-4)$	γC_8H_{14}
31	799 (w)	oop	796 (w)	804	12	oop	$S_{26}(54) - S_{32}(20) + S_{31}(12) - S_{20}(11)$	τ(6-ring)
32	760 (vw)	−23 ± 6	760 (vvw)	764	11	−64	$S_{29}(35) - S_{14}(16) + S_3(14) + S_{24}(13)$	δ(5-ring)
33			700 (vw)	701	0.1	oop	$S_{20}(52) - S_{32}(27) - S_{33}(12) - S_{28}(9)$	γC_6N_{10}
34	690 (vw)	−19 ± 6	691 (w)	685	26	−15	$S_5(19) + S_{14}(15) + S_4(14) + S_7(12)$	ν(ring),
35			604 (vw)	624	24	oop	$S_{31}(63) + S_{32}(29) - S_{28}(5) + S_{20}(5)$	τ(5-ring)
36			595 (vvw)	588	13	4	$S_{30}(29) + S_{16}(13) + S_5(10) - S_4(10)$	δ(5-ring)
37				582	7	oop	$S_{27}(40) + S_{26}(27) + S_{32}(14) + S_{20}(13)$	τ(6-ring)
38			553 (w)	555	3	−62	$S_{24}(55) - S_{10}(10) - S_{18}(8) + S_{16}(6)$	δ(6-ring)
39			519 (vvw)	518	5	67	$S_{25}(63) - S_7(6) - S_{14}(6) + S_{18}(6)$	δ(6-ring)
40				504	12	oop	$S_{38}(89) - S_{39}(5)$	τNH_2 (torsional)
41			393 (vvw)	355	9	−82	$S_{16}(50) + S_{18}(29) - S_{30}(5)$	δC_6N_{10}
42				325	5	oop	$S_{28}(26) + S_{33}(19) + S_{27}(17) - S_{22}(17)$	τ(ring)
43				238	1	−36	$S_{18}(41) - S_{16}(12) + S_{24}(11) + S_7(9)$	δN_7C_{15}
44				232	46	oop	$S_{28}(31) + S_{22}(24) - S_{39}(19) - S_{48}(16)$	τ(ring)
45				214	9	oop	$S_{33}(58) - S_{28}(12) + S_{22}(16) + S_{26}(7)$	τ(5/6-ring)
46				181	29	oop	$S_{48}(63) + S_{22}(14) + S_{39}(10) + S_{28}(10)$	τCH_3
47				107	9	oop	$S_{22}(36) + S_{27}(30) + S_{39}(9) + S_{31}(9)$	γN_7C_{15}
48			582 (m)	74	170	oop	$S_{39}(53) - S_{48}(20) + S_{20}(15) + S_{38}(4)$	γNH_2 (wagging)

[a] The abbreviations within parentheses denote relative intensities: vs = very strong, s = strong, m = medium, w = weak, vw = very weak, vvw = very very weak, and sh = shoulder. [b] Preferred experimental transition moment direction relative to the z' axis (Figure 1), see text. Error bars estimated from the uncertainties in the orientation parameters and in the direction of the orientation axis. [c] Calculated transition moment direction relative the z' axis (Figure 1). [d] Total energy distribution (TED).[54] [e] Assignment of fundamentals and tentative assignments of combination bands and overtones. Descriptions according to Table 1. [f] ND = not determined due to too high PVA absorption in the perpendicular component. [g] oop = out-of-plane polarization. mix = mixed in-plane and out-of-plane polarization.

this polar molecule it is necessary to include solvent effects in the calculations. The SCRF spectra will therefore consistently be used as starting points for the assignment of the vibrational transitions.

Vibrational Assignments. The assignments are based on calculated total energy distributions (TEDs), and on observed spectral shifts when comparing the experimental and calculated spectra (not shown) of 7MA-*8,12,13*-d_3, 9MA-*8,12,13*-d_3, and 2A9MP-*8,12,13*-d_3 with the corresponding nondeuterated derivatives.

The IR and Raman spectra of several adenine derivatives have been reported by Lord and Thomas.[7] Our IR spectrum of crystalline 9MA in KBr pellet is nearly identical to that reported in that study except for a few additional transitions that we observe. Based solely on their experimental observations, Lord and Thomas assigned several of the observed vibrations in relatively broad terms of which just a few need to be revised. A more detailed study of the 9MA vibrational spectrum has been reported by Wiórkiewicz-Kuczera and Karplus[10] based on HF/4−21G calculations. Regarding their assignments we

TABLE 5: Comparison of Experimental and Calculated IR Spectra of 9-Methyladenine

exptl[a]				calcd (SCRF DFT(B3LYP)/6-31G(d,p))				
mode	$\tilde{\nu}$(PVA)/ cm^{-1}	δ^b/ deg	$\tilde{\nu}$(KBr)/ cm^{-1}	$\tilde{\nu}$/ cm^{-1}	IR int/ (km/mol)	δ^c/ deg	TED[d]	assignt[e]
			3346 (w)					$2\nu_8 = 3348$
1			3270 (m)	3730	78	−80	$S_{35}(100)$	$\nu_{as}NH_2$
			3243 (w)					$\nu_8 + \nu_{10} = 3248$
2			3102 (s)	3596	113	11	$S_{34}(100)$	ν_sNH_2
3				3253	0.1	19	$S_{13}(99)$	νC_8H_{14}
4				3171	1	oop[f]	$S_{42}(62) - S_{41}(37)$	$\nu_{as}CH_3$
			3050 (vw)					$\nu_{10} + \nu_{12} = 3059$
5			3030 (w)	3164	81	−58	$S_{11}(100)$	νC_2H_{11}
6			2985 (vw)	3135	14	oop	$S_{41}(63) + S_{42}(35)$	$\nu_{as}CH_3$
			2950 (vw)					$2\nu_{13} = 2952$
7			2922 (w)	3063	77	42	$S_{40}(96) - S_{42}(4)$	ν_sCH_3
			2871 (vw)					$2\nu_{14} = 2878$
			2752 (vvw)					$2\nu_{17} = 2752$
			2688 (vvw)					$\nu_{17} + \nu_{20} = 2686$
			2274 (vvw)					$\nu_{22} + \nu_{26} = 2277$
			2108 (vvw)					$2\nu_{26} = 2096$
			2025 (vvw)					$2\nu_{27} = 2044$
			1889 (vvw)					$2\nu_{28} = 1892$
8	1649 (vs)	+23 ± 5	1674 (vs)	1657	1045	24	$S_{36}(30) - S_5(26) + S_{12}(16) + S_{30}(6)$	δ_sNH_2 (scissoring), ν(ring)
9	1603 (s)	+51 ± 5	1603 (vs)	1637	147	−73	$S_3(19) - S_{36}(12) - S_5(11) + S_8(10)$	ν(ring)
10	1577 (m)	−21 ± 5	1574 (m)	1615	23	9	$S_{36}(43) - S_4(17) + S_3(12) - S_1(7)$	ν(ring), δ_sNH_2 (scissoring)
11	1522 (vw)	+21 ± 5	1522 (vvw)	1551	77	21	$S_8(16) - S_{17}(16) + S_{29}(9) - S_{10}(9)$	ν(5-ring)
12	1487 (sh)	−72/−6 ± 5	1485 (w)	1522	3	mix	$S_{44}(40) + S_{46}(25) + S_{45}(6) - S_6(5)$	$\delta_{as}CH_3$,
13	1477 (m)	−6 ± 5	1476 (w)	1510	90	−8	$S_{44}(31) - S_{15}(19) - S_6(13) - S_{12}(9)$	$\delta_{as}CH_3$,
14	1451 (sh)	−68/−10 ± 5	1439 (vw)	1505	77	mix	$S_{46}(56) - S_{44}(16) - S_{15}(6) - S_{47}(5)$	$\delta_{as}CH_3$
15	1425 (w)	−39 ± 5	1420 (w)	1470	9	−49	$S_{43}(48) + S_8(26) + S_{10}(7) - S_3(4)$	δ_sCH_3, ν(5-ring)
16	1413 (w)	−39 ± 5	1411 (w)	1448	61	90	$S_{43}(42) - S_{10}(18) - S_8(10) + S_4(6)$	δ_sCH_3, ν(5-ring)
17	1380 (w)	+36 ± 5	1376 (w)	1406	68	7	$S_{15}(44) + S_6(11) + S_4(10) - S_{12}(9)$	δC_2H_{11}
18	1345 (sh)	−45 ± 5	1351 (w)	1375	86	−57	$S_7(24) - S_9(17) - S_8(14) - S_{17}(9)$	ν(5-ring)
19	1328 (m)	−33 ± 5	1327 (w)	1358	13	87	$S_1(34) + S_9(15) - S_{12}(10) - S_{14}(6)$	ν(ring)
20	1305 (m)	+43 ± 5	1310 (m)	1353	162	46	$S_2(48) - S_3(9) + S_9(7) + S_{23}(6)$	ν(6-ring)
21	1255 (sh)	+38 ± 5	1256 (w)	1287	94	44	$S_{37}(22) + S_7(12) - S_{14}(11) - S_1(10)$	$\delta_{as}NH_2$ (rock), ν(ring)
22	1236 (m)	+14 ± 5	1229 (m)	1261	110	5	$S_{17}(37) + S_8(13) - S_9(9) + S_1(7)$	δC_8H_{14}
23	1196 (vw)	−5 ± 5	1200 (w)	1229	4	−19	$S_{17}(19) + S_7(15) - S_2(12) + S_{29}(11)$	ν(5-ring)
24			1094 (sh)	1153	5	42	$S_{45}(52) + S_{47}(39) - S_{44}(5)$	$\delta_{as}CH_3$
25			1085 (w)	1089	13	55	$S_{37}(15) - S_{47}(12) + S_{45}(10) + S_{30}(9)$	$\delta_{as}CH_3$, $\delta_{as}NH_2$ (rock)
26	1053 (vw)	−43 ± 5	1048 (m)	1066	37	−45	$S_9(19) + S_{47}(17) + S_{45}(12) + S_{37}(10)$	ν(5-ring), $\delta_{as}CH_3$
27	1007 (vw)	+8 ± 5	1022 (w)	1018	51	31	$S_{37}(26) - S_6(26) + S_{12}(11) - S_{30}(10)$	ν(ring), $\delta_{as}NH_2$ (rock)
28	954 (vw)	oop[f]	946 (w)	963	2	oop	$S_{19}(108) - S_{27}(-5) - S_{26}(-4)$	γC_2H_{11}
29	905(vw)	−65 ± 5	904 (vw)	908	14	−76	$S_{23}(49) + S_{30}(10) - S_4(10) - S_7(9)$	δ(ring)
30	837 (vw)	oop	843 (w)	865	4	oop	$S_{21}(98)$	γC_8H_{14}
31	798 (w)	oop	797 (m)	808	13	oop	$S_{26}(51) + S_{31}(22) - S_{20}(19) + S_{21}(6)$	τ(ring)
32	745 (w)	+7 ± 5	743 (w)	748	11	−5	$S_{14}(21) + S_{24}(20) - S_{30}(10) + S_4(10)$	δ(ring), $\nu N_9 C_{15}$
33	721 (m)	+16 ± 5	720 (m)	733	36	18	$S_{29}(30) + S_3(14) + S_5(12) + S_7(7)$	δ(ring)
34			683 (w)	687	4	oop	$S_{20}(48) - S_{32}(15) - S_{28}(14) - S_{33}(13)$	γC_6N_{10}
35	648 (w)	oop	638 (vvw)	659	39	oop	$S_{31}(55) + S_{32}(33) - S_{26}(8) + S_{33}(6)$	τ(5-ring)
36	595 (vw)	+23 ± 5	603 (w)	595	9	−3	$S_{30}(19) + S_{16}(19) - S_{29}(15) + S_5(12)$	δ(5-ring)
37			557 (vvw)	569	2	oop	$S_{27}(40) + S_{32}(30) + S_{26}(24) + S_{20}(12)$	τ(ring)
38			542 (vw)	539	7	−66	$S_{25}(29) - S_{24}(20) + S_{14}(11) - S_{18}(10)$	δ(6-ring)
39	537 (vw)	+17 ± 5	530 (vw)	532	16	24	$S_{25}(48) + S_{24}(27) + S_4(7)$	δ(6-ring)
40	479 (vvw)	oop		500	20	mix	$S_{38}(92)$	τNH_2 (tors)
41			690 (m)	372	510	mix	$S_{39}(94) - S_{36}(-6) + S_{33}(6)$	γNH_2 (wagging)
42			357 (w)	311	20	mix	$S_{16}(43) - S_{18}(31) - S_5(5) - S_{30}(4)$	δC_6N_{10}
43			312[g]	308	15	oop	$S_{28}(45) + S_{27}(15) - S_{32}(10) + S_{31}(9)$	τ(6-ring)
44			245[g]	248	14	oop	$S_{33}(47) - S_{22}(33) + S_{20}(6)$	τ(5/6-ring)
45			208[h]	218	20	−90	$S_{18}(39) - S_{24}(16) + S_{16}(16) + S_{10}(7)$	δN_9C_{15}
46			157/135[h]	199	1	oop	$S_{28}(37) - S_{22}(20) - S_{27}(19) - S_{33}(18)$	τ(6-ring)
47				111	14	oop	$S_{22}(31) - S_{27}(29) + S_{26}(12) + S_{20}(7)$	γN_9C_{15}
48				42	0.06	−87	$S_{48}(91) + S_{22}(10)$	τCH_3

[a] The abbreviations within parentheses denote relative intensities: vs = very strong, s = strong, m = medium, w = weak, vw = very weak, vvw = very very weak, and sh = shoulder. [b] Preferred experimental transition moment direction relative to the z' axis (Figure 1), see text. Error bars estimated from the uncertainty in the direction of the orientation axis. [c] Calculated transition moment direction relative the z' axis (Figure 1). [d] Total energy distribution (TED).[54] [e] Assignment of fundamentals and tentative assignments of combination bands and overtones. Descriptions according to Table 1. [f] oop = out-of-plane polarization. mix = mixed in-plane and out-of-plane polarization. [g] Raman spectrum of polycrystalline 9MA reported by Savoie *et al.*[8] [h] Raman spectrum of polycrystalline 9MA reported by Harada and Lord.[11]

propose some reassignments which will be discussed below. We are not aware of any reports on IR spectra of 7MA and 2A9MP and will therefore discuss the fundamental transitions of the three compounds together, and with one characteristic spectral region at a time. The experimental material is summarized in Table 4 for 7MA, Table 5 for 9MA, and Table 6 for 2A9MP.

(i) Region from 3400 to 2900 cm^{-1}. For the solid state samples (KBr), several transitions due to NH and CH stretchings are observed in this region. In the case of the samples in PVA

TABLE 6: Comparison of Experimental and Calculated IR Spectra of 2-Amino-9-methylpurine

exptl[a]				calcd (SCRF DFT(B3LYP)/6-31G(d,p))				
mode	$\tilde{\nu}$(PVA)/ cm^{-1}	δ^b/ deg	$\tilde{\nu}$(KBr)/ cm^{-1}	$\tilde{\nu}$/ cm^{-1}	IR int/ (km/mol)	δ^c/ deg	TED[d]	assignt[e]
			3391 (s)					$\nu_{as}NH_2$ (non H-bonded)
1			3303 (s)	3740	73	34	$S_{35}(100)$	$\nu_{as}NH_2$
			3257 (vvw)					$\nu_8 + \nu_9 = 3255$
2			3192(s)	3607	146	−61	$S_{34}(100)$	ν_sNH_2 (non H-bonded)
			3167 (sh)					ν_sNH_2
3			3087 (w)	3247	1	−68	$S_{13}(99)$	νC_8H_{14}
4			3068(vvw)	3174	1	oop[g]	$S_{42}(76) - S_{41}(20)$	$\nu_{as}CH_3$
			3050 (vvw)					$2\nu_{11} = 3058$
5			3017	3154	68	8	$S_{12}(100)$	νC_6H_{11}
6				3137	14	oop	$S_{41}(78) + S_{42}(22)$	$\nu_{as}CH_3$
7			2924 (vw)	3065	66	49	$S_{40}(97)$	ν_sCH_3
			2724 (vvw)					$\nu_{16} + \nu_{19} = 2728$
			1922 (vvw)					$2\nu_{27} = 1920$
			1848 (vvw)					$2\nu_{28} = 1852$
			1811 (vvw)					$\nu_{28} + \nu_{29} = 1812$
			1762 (vw)					$2\nu_{29} = 1772$
8	1640 (sh)	69 ± 7	1635 (vs)	1667	395	−89	$S_3(30) - S_5(14) + S_6(12) - S_{10}(7)$	ν(6-ring),
9	1617 (s)	−69 ± 8	1620/1611 (s)	1636	698	−67	$S_{36}(75) + S_{11}(15)$	δ_sNH_2 (scis.)
10	1582 (s)	20 ± 7	1585 (s)	1616	222	4	$S_5(24) - S_4(18) + S_3(11) - S_1(11)$	ν(6-ring)
11	1529 (m)	−41 ± 7	1529 (m)	1567	64	−8	$S_8(21) - S_{17}(15) - S_{10}(13) + S_{36}(7)$	ν(5-ring)
12				1517	36	mix	$S_{46}(75) - S_{47}(10) + S_{44}(5)$	$\delta_{as}CH_3$
13				1507	16	oop	$S_{44}(84) + S_{45}(8) - S_{46}(7)$	$\delta_{as}CH_3$
14	1470 (m)	−78 ± 7	1476 (m)	1501	122	−72	$S_8(14) - S_{30}(12) + S_{11}(10) + S_{10}(10)$	ν(5-ring)
15	1439 (s)	−66 ± 8	1442 (s)	1474	213	−78	$S_{43}(52) + S_2(9) + S_8(8) - S_{11}(7)$	δ_sCH_3
16	1414 (m)	49 ± 7	1415 (m)	1447	451	−82	$S_{43}(38) + S_{16}(11) + S_{11}(10) - S_{10}(7)$	δ_sCH_3
17	1375 (w)	54 ± 7	1383 (w)	1412	39	62	$S_6(19) - S_8(17) + S_5(9) + S_{14}(8)$	ν(ring)
18	1332 (w)	2 ± 10	1333 (vw)	1365	6	81	$S_8(16) - S_7(15) - S_9(13) + S_{16}(11)$	ν(5-ring)
19	1309 (sh)	−85 ± 13	1308 (vw)	1336	191	−83	$S_6(19) - S_8(17) + S_5(9) - S_3(9)$	ν(6-ring)
20	1294 (w)	60 ± 8	1294 (m)	1331	21	−18	$S_{16}(24) - S_9(19) + S_{47}(12) + S_{10}(11)$	δC_6H_{11}
21	1250 (w)	−52 ± 7	1250 (w)	1291	55	−11	$S_{16}(20) + S_7(17) + S_9(11) - S_3(9)$	ν(5-ring)
22	1208 (w)	−26 ± 7	1204 (vw)	1234	32	−22	$S_{17}(43) + S_{14}(12) + S_7(10) - S_4(9)$	δC_8H_{14}
23			1127 (sh)	1152	2	73	$S_{45}(76) + S_{47}(14) - S_{44}(7)$	$\delta_{as}CH_3$
24			1116 (vw)	1146	13	−45	$S_{23}(22) - S_{14}(21) + S_4(12) + S_5(7)$	δ(6-ring)
25			1097 (sh)	1104	17	−53	$S_{37}(43) + S_2(21) + S_{47}(11) - S_{10}(6)$	$\delta_{as}NH_2$ (rock)
26	1047	ND[f]	1057 (vw)	1061	28	−53	$S_{47}(30) + S_9(27) + S_{29}(12) - S_{45}(6)$	$\delta_{as}CH_3$
27	963 (w)	29 ± 7	960 (w)	974	49	46	$S_1(38) + S_{11}(10) - S_{37}(10) - S_{10}(7)$	ν(6-ring)
28	915 (vw)	oop[g]	926 (vw)	964	7	oop	$S_{20}(103)$	γC_6H_{11}
29	855 (vw)	oop	848 (vw)	863	3	oop	$S_{21}(99)$	γC_8H_{14}
30	889 (vw)	−16/10 ± 8	886 (vw)	854	9	mix	$S_{23}(32) + S_{30}(18) - S_7(17) - S_4(14)$	δ(ring)
31	797 (w)	oop	793 (m)	809	24	oop	$S_{26}(52) - S_{19}(23) + S_{31}(14) + S_{21}(5)$	τ(6-ring)
32	789 (vw)	35 ± 7	785 (sh)	809	35	37	$S_{25}(17) + S_{30}(12) + S_{29}(11) + S_1(10)$	δ(ring)
33			733 (vvw)	736	11	oop	$S_{19}(39) + S_{31}(28) - S_{27}(13) - S_{32}(8)$	γC_2N_{11}
34			712 (vvw)	712	10	32	$S_{14}(23) + S_{24}(22) - S_{29}(12) + S_4(10)$	δ(ring)
			679 (vvw)					δ(5-ring)
35	631 (w)	oop	631 (m)	643	22	oop	$S_{32}(57) + S_{31}(39) + S_{33}(8) + S_{21}(-5)$	τ(5-ring)
36			614 (vvw)	608	6	−12	$S_{29}(23) - S_{30}(21) + S_{15}(14) - S_5(11)$	δ(5-ring)
37				541	6	9	$S_{25}(27) + S_{24}(20) - S_{10}(9) + S_{18}(7)$	δ(6-ring)
38			495 (vw)	502	43	−59	$S_{25}(28) - S_{24}(25) + S_{38}(16) - S_7(8)$	δ(6-ring)
39				481	24	oop	$S_{38}(69) - S_{25}(5) + S_{24}(6) + S_{18}(5)$	τNH_2 (torsional)
40			417 (vw)	454	47	oop	$S_{28}(52) + S_{19}(18) + S_{26}(17) + S_{39}(6)$	τ(6-ring)
41			513 (w)	401	492	oop	$S_{39}(71) - S_{28}(9) + S_{15}(7)$	γNH_2 (waggin)
42				373	114	79	$S_{15}(46) + S_{18}(13) + S_{38}(11) - S_{39}(9)$	δC_2N_{10}
43				358	30	oop	$S_{32}(25) - S_{33}(23) + S_{26}(20) - S_{28}(12)$	τ(ring)
44				261	1	oop	$S_{33}(36) - S_{22}(33) - S_{28}(18) - S_{27}(8)$	τ(ring)
45				220	10	−65	$S_{18}(53) + S_{10}(9) - S_{24}(9) - S_{15}(8)$	δN_9C_{15}
46				155	10	oop	$S_{22}(35) - S_{33}(35) + S_{28}(17) + S_{27}(9)$	γN_9C_{15}
47				131	0.3	oop	$S_{27}(56) - S_{22}(26) - S_{32}(10) + S_{31}(4)$	τ(6-ring)
48				28	0.02	mix	$S_{48}(92) + S_{22}(9)$	τCH_3

[a] The abbreviations within parentheses denote relative intensities: vs = very strong, s = strong, m = medium, w = weak, vw = very weak, vvw = very very weak, and sh = shoulder. [b] Preferred experimental transition moment direction relative to the z' axis (Figure 1), see text. Error bars estimated from the uncertainties in the orientation parameters and in the direction of the orientation axis. [c] Calculated transition moment direction relative the z' axis (Figure 1). [d] Total energy distribution (TED).[54] [e] Assignment of fundamentals and tentative assignments of combination bands and overtones. Descriptions according to Table 1. [f] Not determined due to too high PVA absorption in the perpendicular component. [g] oop = out-of-plane polarization. mix = mixed in-plane and out-of-plane polarization.

film, the strong background absorption prevented us from observing any transitions above 1800 cm^{-1}.

For 7MA, the two relatively strong peaks at 3325 and 3125 cm^{-1} are assigned to the asymmetric stretch (ν_1) and symmetric stretch (ν_2) NH_2 vibrations, respectively. They shift to 2515 and 2342 cm^{-1} for 7MA-*8,12,13-d*$_3$.

For 9MA the asymmetric stretch is observed at 3270 cm^{-1} and the symmetric stretch at 3102 cm^{-1}. Wiórkiewicz-Kuczera and Karplus[10] assigned the asymmetric and symmetric stretches to the weak 3355 cm^{-1} and medium intensity 3280 cm^{-1} Raman bands observed by Savoie *et al.*[8] The higher frequency band is observed in the IR at 3346 cm^{-1} and is assigned to the first

overtone of ν_8. The shifts to 2465 and 2294 cm^{-1} and the similar intensity pattern upon deuteration clearly supports our assignments of ν_1 and ν_2. In the case of 2A9MP, three strong bands attributed to NH_2 stretchings are observed. The first two at 3391 and 3303 cm^{-1} we believe correspond to the asymmetric stretching where the first component is proposed to stem from a "less" hydrogen-bonded molecule in the crystal while the second component arises from a "more" hydrogen-bonded amino group. The third peak is observed at 3197 cm^{-1} and has a shoulder at 3167 cm^{-1}. These features correspond to the two components of the symmetric stretch. The asymmetric ND_2 stretch is observed at 2552/2498 cm^{-1} and the symmetric stretch at 2385/2336 cm^{-1}.

The νC_8H (νC_8D) modes are observed at 3081 cm^{-1} (2293 cm^{-1}) and at 3087 cm^{-1} (2304 cm^{-1}) for 7MA and 2A9MP, respectively. The corresponding vibrations are not observed for 9MA and are probably hidden by the strong symmetric NH_2/ND_2 stretch vibrations. The νC_2H modes of 7MA and 9MA are assigned to the bands at 2976 cm^{-1} and at 3030 cm^{-1}, respectively. The νC_6H of 2A9MP is assigned to the very weak band at 3017 cm^{-1}.

The CH stretchings of the methyl groups are observed in the 3070−2900 cm^{-1} region. Splittings of the symmetric CH_3 stretch vibration are observed for all compounds, probably due to Fermi resonances with combination bands of the CH_3 deformation vibrations.[58]

(ii) Region from 1700 cm^{-1} to 1550 cm^{-1}. In this region each of three molecules have three strong vibrations of which one is mainly due to NH_2 scissoring and the remaining two are mainly due to stretchings in the 6-membered ring with contributions from NH_2 scissoring. The NH_2 (ND_2) scissoring vibrations are assigned to the bands observed in the solid state at 1666 cm^{-1} (1195 cm^{-1}), 1674 cm^{-1} (1186 cm^{-1}), and at 620/1610 cm^{-1} (not observed) for 7MA, 9MA, and 2A9MP, respectively. In analogy with the observation for the NH_2 stretchings, the NH_2 scissoring of 2A9MP in the solid state is split into two components. The ring stretches of 7MA are observed at 1612 and 1560 cm^{-1}, at 1603 and 1577 cm^{-1} for 9MA, and at 1610 and 1582 cm^{-1} for 2A9MP. The 1577 and 1582 cm^{-1} vibrations of 9MA and 2A9MP, as well as the 1560 cm^{-1} vibration of 7MA, seem to be characteristic of 9-substituted and 7-substituted purines, respectively. The corresponding transitions are found at 1584 cm^{-1} for 9-methylpurine and at 1568 cm^{-1} for 7-methylpurine.[41]

(iii) Region from 1550 cm^{-1} to 1200 cm^{-1}. Several bands observed between 1490 and 1400 cm^{-1} are assigned to CH_3 deformation vibrations. The medium to strong intensity bands at 1479 and 1401 cm^{-1} in the spectrum 7MA are assigned to ring stretch vibrations. The 1328 and 1305 cm^{-1} bands of 9MA are observed also for Ado which supports the assignment that they are ring-stretching vibrations. For 2A9MP, the bands at 1524 and 1333 cm^{-1} are assigned to stretchings in the 5-membered ring. The corresponding bands of 2APr are observed at 1516 and 1335 cm^{-1}. The δC_6H of 2A9MP and 2Apr is assigned to the band at about 1294 cm^{-1}. The δC_8H (δC_8D) vibrations have been confidently assigned for all three derivatives to the bands observed at 1235 cm^{-1} (945 cm^{-1}), 1229 cm^{-1} (932 cm^{-1}), and 1204 cm^{-1} (916 cm^{-1}) for 7MA, 9MA, and 2A9MP, respectively.

(iv) Region from 1200 cm^{-1} to 450 cm^{-1}. Several in-plane and out-of-plane deformation vibrations of the purine ring system and the NH_2 rocking vibrations are assigned to bands between 1200 and 450 cm^{-1}. Also found here are the bands due to CH out-of-plane bending vibrations. In a previous study of the polarized IR spectrum of 9MA crystals, Kyogoku *et al.*[5] assigned five bands in the region to out-of-plane vibrations. Our experiments confirm these assignments.

For each molecule we expect two out-of-plane CH bending (γCH) modes. The γC_2H of 7MA is assigned to the very weak band at 970 cm^{-1} observed only for 7MA in the solid state, and the γC_8H is assigned to the shoulder at 875 cm^{-1} in PVA that has out-of-plane polarization. In the case of 9MA, the γC_2H is assigned to the 954 cm^{-1} out-of-plane polarized band observed by us and Kyogoku *et al.*[5] at 946 cm^{-1} for crystalline 9MA. At 837 cm^{-1} (843 cm^{-1} in KBr), the γC_8H is observed. For 9MA-*8,12,13-d*$_3$, this band shift to the very weak band observed at 725 cm^{-1} (KBr). The γC_6H and γC_8H modes are assigned to the out-of-plane-polarized bands at 915 and 848 cm^{-1}. The γC_8D of 2A9MP-*d*$_3$ is assigned to the band at 727 cm^{-1}.

The bands at 799 cm^{-1} (7MA), 798 cm^{-1} (9MA), and 797 cm^{-1} (2A9MP) are all assigned to a pyrimidine torsion vibration related to the out-of-plane deformation vibration observed at about 700 cm^{-1} for benzene derivatives.[59] The out-of-plane-polarized bands at 648 cm^{-1} for 9MA and at 631 cm^{-1} for 2A9MP are assigned to the torsion of the 5-membered ring. For 7MA, this vibration is not observed at all in PVA film but at 604 cm^{-1} in KBr.

Finally, we discuss the wagging and torsion vibrations of the amino group. The NH_2 and ND_2 wagging vibrations are expected to be strongly anharmonic in analogy with the NH_2 wagging vibrations of ammonia and aniline[60] which makes an analysis based on harmonic motion nonvalid. In the case of 9MA in the solid state, the relatively broad band at 690 cm^{-1} has been assigned to the to the NH_2 wagging vibration.[5,7] Upon deuteration of the amino group, this band disappears and a new band appears at 490 cm^{-1} similar in shape and intensity to the band at 690 cm^{-1} for 9MA. These two bands probably correspond to one or several components of the NH_2 and ND_2 wagging vibrations, respectively. The NH_2 wagging vibration of 9MA is predicted at 372 cm^{-1} in the SCRF calculation and at 265 and 236 cm^{-1} in the gas-phase calculation. The frequency of this vibration is obviously extremely sensitive to the amino group pyramidalization and, therefore, it is expected to be difficult to appropriately model this vibration for 9MA in the condensed phase. For 7MA and 2A9MP in the solid state, the respective bands at 584 and 513 cm^{-1} are assigned to the NH_2 wagging vibrations. They shift to 428 and 387 cm^{-1}, respectively, for the N-deuterated compounds. For 9MA and 9MA-*8-d* in PVA film we observe a very weak out-of-plane-polarized band at 479 cm^{-1} that might be due to the NH_2 wagging or the NH_2 torsion predicted at 500 cm^{-1}. The NH_2 torsions of 7MA and 2A9MP predicted at 504 and 481 cm^{-1}, respectively, are not observed, we believe, in either PVA film or KBr.

(v) Region below 450 cm^{-1}. The very weak IR band observed at 357 cm^{-1} for 9MA is assigned to the δC_6N_{10} mode. This band was reported by Lord and Thomas[7] to shift to 337 cm^{-1} in the Raman spectrum of 9MA-*12,13-d*$_2$. The shift is consistent with the 2 au increase of the mass of the amino group. For 7MA the δC_6N_{10} mode is assigned to the band observed at 393 cm^{-1}. In the case of 2A9MP there is a very weak band observed at 417 cm^{-1} that could be due to δC_2N_{10} or the ring mode predicted at 454 cm^{-1}.

Harada and Lord[11] have studied the IR and Raman spectra of 9MA and 9MA-*12,13-d*$_2$ in the solid state below 225 cm^{-1}. They assigned the IR bands of 9MA observed at 208 cm^{-1} and 155/135 cm^{-1} to out-of-plane ring deformation vibrations and bands observed at even lower frequencies were assigned to lattice modes. On the basis of the calculated spectrum of 9MA,

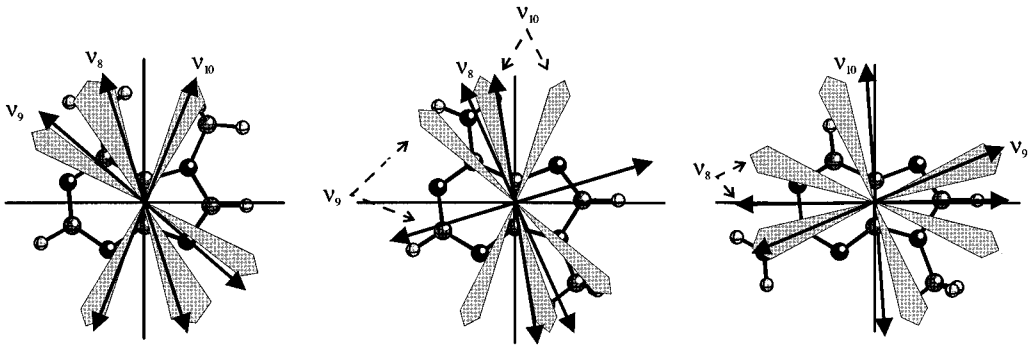

Figure 8. Experimental (shaded arrows) and calculated (black arrows) IR transition moment directions for the modes ν_8, ν_9, and ν_{10} in 7MA, 9MA, and 2A9MP. The width of the shaded arrows indicate the experimental uncertainties including the estimated uncertainties in the orientation axes directions (±5°).

the 205 cm^{-1} band is assigned to the in-plane bending of the of the methyl group and the bands at 155/135 cm^{-1} to a ring torsion vibration.

IR Transition Moments. For each in-plane transition, there are two possible values of the angle δ, and it is not possible *a priori* to distinguish between these. An experimental approach to solve this sign ambiguity is to vary the substituents on the molecules thereby rotating the orientation axis direction and correlating the subsequent changes of the IR polarizations with respect to sign of the rotation of the orientation axis. This can only be done for vibrations that not are affected in their nature by the change of substituent and thus are observed at about the same frequency and with similar intensity regardless of the substituent. In the case of 9MA and 2A9MP, this strategy has been employed by the use of their respective 9-substituted ribose derivatives adenosine (Ado) and 2-aminopurine riboside (2APr) (Figure 3, Table 1S). For 9MA, the vibrations that were compared with those observed for Ado were ν_8, ν_9,ν_{10}, ν_{19}, and ν_{20}. These modes have either NH_2 scissoring or ring stretching character and, thus, they are expected to be relatively insensitive to the change of substituent in the ninth position. The changes in the relative angles between the transition moment directions and the orientation axis when going from 9MA to Ado ranges from 0° to −12° with a −6° average realignment of the orientation axis (Table 3). For 2A9MP, ν_8, ν_9,ν_{10}, ν_{18}, and ν_{20} were investigated (Table 6). The average realignment of the orientation axis for 2APr is found to be −10° compared with that of 2A9MP (Table 3). Although being only one example of variation of substituent, these observed rotations are all consistent with the expected elongation of the purine ring system along its short axis upon ribose substitution[61] and with the fact that the effective size of realignment is mainly determined by the size of the angle between the original orientation axis of the methylated derivative and the glycosidic bond of the ribose derivative. The concluded experimental polarizations, after discarding one of the two possible angles δ, are thus found to be the most plausible ones and the majority of them are also in good agreement with calculated polarizations (*vide infra*) (Tables 5 and 6). In addition, we conclude that the polarizations examined in this way are transferable from 9MA and 2A9MP to Ado and 2APr, respectively, which can be important for the use of the determined IR polarizations at the interpretation of VCD or IR LD measurements on nucleic acids containing adenine or 2-aminopurine bases.

An alternative approach to solve the sign ambiguity problem is to rely on *ab initio* calculated polarizations to guide the choice of the correct experimental polarization. A drawback of such a procedure is the relatively large uncertainty in the calculated polarizations. In a recent study by Radziszewski *et al.*[21] of the IR polarizations of propene and some deuterated propenes oriented in stretched polyethylene sheets, it was found that even for the high-level CCSD/6-311G(d,p) calculations, the expected error margin for the calculated polarizations is generally about ±20° and for some weak transitions considerably more.[62]

The calculated polarizations were used in the case of all in-plane vibrations for 7MA and also for the majority of the in-plane vibrations of 9MA and 2A9MP. The root-mean-square (RMS) differences between all experimental and corresponding calculated polarizations for the three compounds are as follows for the SCRF and gas-phase calculations, respectively: 7MA, 13° and 20°; 9MA, 16° and 20°; and 2A9MP, 25° and 26°.

Those transitions, for which there is a 30° or larger difference between experimental and calculated polarizations, are in most cases found experimentally to be weak or in a few cases calculated to be weak which could explain why their polarizations deviate from experiment.[21] In one case also a strong transition was found to have a polarization that varied between experiment and theory: ν_9 of 9MA is experimentally found to be polarized closely parallel to the orientation axis (51°) but is predicted both in the DFT(B3LYP) and MP2 calculations to have a polarization of about −73°. This vibration has a calculated predominance of ring stretching motion but it has also a considerable contribution of NH_2 scissoring. The reason for the large difference between experimental and calculated polarizations is probably that the calculated mixing of ring stretching and scissoring motions is not the correct one. This conclusion is supported by that the same ring-stretching vibration is calculated[63] to occur in 9-methylpurine with a polarization of +63° and that it is observed in PVA film at the same frequency, 1603 cm^{-1}, as it is for 9MA and with an possible experimental polarization of +65°.[41] Specific environmental effects such as hydrogen bonding could be an origin of a perturbed mixing of internal coordinates and thus the polarization for this vibration. Furthermore, inadequacies of the computational method as well as anharmonic effects could at least in part be responsible for the the observed deviation. We have however not investigated this further since the main issue of this work is to provide reliable experimentally determined IR polarizations.

The final choices of experimental in-plane polarizations are presented in Tables 4, 5, and 6. The error bars for the polarizations contain both the uncertainty in the orientation parameters and the uncertainty in the position of the orientation axis.

The experimental and calculated polarizations for the strong NH_2 scissoring and ring-stretching vibrations ν_8, ν_9, and ν_{10} are displayed in Figure 8.

Tautomerism. From temperature-jump relaxation measurements on adenine in aqueous solution, the $\Delta H°$ and $\Delta S°$ for the 9-H-adenine/7-H-adenine equilibrium (Figure 9) have been determined to be 0.88 ± 0.08 kJ/mol and −7.6 ± 0.5 J/(mol

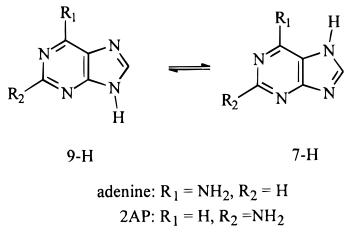

Figure 9. The 9-H/7-H tautomeric equilibrium of adenine and 2AP.

K), respectively, corresponding to a $\Delta G° = 3.15$ kJ/mol or a relative 7-H-adenine concentration of 22% at 25 °C.[17]

In this work we have examined the isotropic absorbance spectra of adenine and 2AP in PVA film in order to search for spectral inhomogeneities that could be attributed to the presence of the minor 7-H tautomeric form. The spectra have been examined in the frequency range 1700−450 cm^{-1}. However, due to the relatively low resolution of the vibrational bands in a PVA film, and the expected overlap between bands that stem from different tautomeric forms, it was only the bands in the less congested 1700−1540 cm^{-1} region that were used in a quantitative analysis.

The observed isotropic absorption spectrum of adenine in PVA is clearly not due to a single spectroscopic species. The adenine band centered around 1651 cm^{-1} is markedly broader compared to the bands of 7MA and 9MA, and the band centered at 1600 cm^{-1} is also broader with a slight shoulder at 1590 cm^{-1}. Finally, the 1560 cm^{-1} band (ν_{10}) characteristic of 7MA is also present in the adenine spectrum although weaker than in 7MA (Figure 3a). The calculated frequencies and intensities of 7-H-adenine and 9-H-adenine (Figure 3b) in the 1700−1550 cm^{-1} region are very similar to those of 7MA and 9MA, respectively. Assuming that that the molar absorptivities of the 1560 cm^{-1} vibration are the same in 7-H-adenine and 7MA, the observed intensity corresponds to an 7-H-adenine content of 23 ± 3%, in good agreement with previous determinations.[17] The uncertainty is due to the experimental difficulties in the preparation of the PVA films of identical thicknesses and concentrations.

Previously, we have computationally investigated the 7-H/9-H tautomeric equilibrium of purine, adenine, and 2-aminopurine at the SCRF MP2/6-31G(d)/MP2/6-31G(d) level.[29] In comparison with the available experimental data for 7-H/9-H tautomeric equilibrium of adenine[17,18] and purine[19] in room temperature aqueous solution, we found that a strictly empirical 3kJ/mol reduction of the calculated ΔE (at 0 K) = $E_{7-\text{H taut}} - E_{9-\text{H taut}}$ yielded for both purine ($\Delta E = 2.97$ kJ/mol) and adenine ($\Delta E = 6.77$ kJ/mol), $\Delta G°$ values in good agreement with experiment. Assuming that the computational error was the same for 2AP ($\Delta E = 11.2$ kJ/mol), we predicted that the relative 7-H-2AP content should be about 3% in room temperature aqueous solution. As a test of the DFT method, we performed SCRF DFT(B3LYP/6-31G(d,p)//DFT(B3LYP)/6-31G(d,p) calculations and we obtained the following ΔE values for the 7-H and 9-H tautomers of adenine and 2AP, respectively: 4.8 and 13.6 kJ/mol, which are quite similar to the MP2 results.[29] By contrast, when the geometries of the 7-H and 9-H forms of adenine are optimized in SCRF DFT(B3LYP)/6-31G(d,p) calculations, the ΔE for adenine is reduced to 0.27 kJ/mol at 0 K, due to the large stabilization of the 7-H tautomer in the reaction field, and after thermal corrections to enthalpies and free energies, we obtained a $\Delta H = -0.48$ kJ/mol and a $\Delta G = -3.49$ kJ/mol at 20 °C. In the case of 2AP we obtain a $\Delta H = 12.2$ kJ/mol and a $\Delta G = 12.6$ kJ/mol. However, it has recently been shown by Foresman *et al.*[64] that conformational energies obtained with the simple SCRF model are in most cases in qualitative agreement with experimental energies but are not as accurate as energies obtained from more sophisticated continuum models such as the polarized-continuum model (PCM) developed by Tomasi and co-workers.[49] We applied the PCM method and obtained a $\Delta G = -5.06$ kJ/mol for the SCRF optimized geometries (eq 7). For 2AP, the corresponding value is 15.0 kJ/mol. Both the SCRF and the PCM methods yield ΔG values for adenine which are of about 6−8 kJ/mol too low, leading to an erroneous stabilization of the 7-H tautomer of adenine. This is probably due to an combination of the errors due to the relatively low level of computational method and, probably more important, to the lack of specific solvent effects in the continuum methods. Interesting to note is that the SCRF ΔH value for adenine is only of 1.36 kJ/mol from that measured by Dreyfus *et al.*,[17] and if it is assumed that this error is the same for the 2AP tautomers and that the entropic contribution is the same as measured for adenine,[17] we predict a relative amount of the 7-H tautomer of 2AP of less than 1% at 25° C.

The isotropic spectra of 2AP, 2A9MP, and 2APr in the 1700−1550 cm^{-1} region are displayed in Figure 4a. The band in 2A9MP at 1610 cm^{-1}, which is assigned to the NH_2 scissoring vibration (Table 6), is clearly blue shifted for 2AP. The cause of this shift can be a change in the hydrogen bonding pattern for 2AP compared to the two 9-substituted derivatives or that the 2AP exists as a mixture of the 7-H and 9-H tautomers. The calculated IR spectra of 9-H-2AP and 2A9MP in the discussed region are very similar but now also the calculated IR spectra of 7-H-2AP and 9-H-2AP (Figure 4b) are more similar to each other, in contrast to the case of the adenine tautomers and, therefore, it is expected that it will be difficult to observe any characteristic feature belonging to the supposed minor 7-H tautomer in the low-resolution IR spectrum of 2AP in PVA.

Conclusions

The IR spectra of 7MA, 9MA and 2A9MP have been characterized in terms of transition energies, intensities, and transition moment directions both experimentally and computationally. Five characteristic in-plane vibrations have been identified both for the 9-substituted adenine chromophore and the 9-substituted 2-aminopurine chromophore. Thus, the polarizations determined for these vibrations are expected to be useful in the interpretation of IR LD and VCD spectra of nucleic acids containing adenine or 2-aminopurine bases.

The agreement between experimental and calculated IR polarizations is generally improved when going from the gas-phase calculations to the SCRF calculations. The improvement is especially pronounced for 7MA with an RMS difference between experimental and calculated in-plane polarizations of only 13°. Thus, the SCRF DFT(B3LYP)/6-31G(d,p) geometry of 7MA is probably a good description of the structure of 7MA in a polar solvent.

Previous estimates of the abundance of the 7-H-adenine tautomer in polar solvents are confirmed by comparison of the spectrum of adenine in PVA film with the spectra of 7MA and 9MA. The relative amount of 7-H-adenine in the PVA matrix was determined to be 23 ± 3%.

Acknowledgment. The Swedish Natural Science Research Council (NFR) is acknowledged for financial support. Professor Jacopo Tomasi is acknowledged for providing the PCM routine. Professor Wesley D. Allen is acknowledged for providing the INTDER95 code (ref 52). I am grateful to Professor Bengt Nordén for his critical reading of the manuscript. Drs. Bo Albinsson and Anders Broo are acknowledged for valuable discussions.

Supporting Information Available: Tabulated IR spectra of Ado, 2APr, adenine, and 2AP in PVA film (Table 1S). MP2/

6-31G(d) IR spectrum of 9MA (Table 2S). DFT(B3LYP)/6-31G(d,p) IR spectra of 7MA, 9MA, and 2A9MP (Tables 3S, 4S, and 5S, respectively). DFT(B3LYP)/6-31G(d,p) IR spectra of the propenes investigated by Radziszewski *et al.*[21] (Table 6S) (7 pages). Ordering information is given on any current masthead page.

References and Notes

(1) Annamalai, A.; Keiderling, T. A. *J. Am. Chem. Soc.* **1987**, *109*, 3125. Wang, L.; Keiderling, T. A: *Biochemistry* **1992**, *31*, 10265. Yang, L.; Keiderling, T. A. *Biopolymers* **1993**, *33*, 315. Wang, L.; Keiderling, T. A. *Nucleic Acids Res.* **1993**, *21*, 4127. Wang, L.; Yang, L.; Keiderling, T. A. *Biophys. J.* **1994**, *67*, 2460. Wang, L.; Pancoska, P.; Keiderling, T. A. *Biochemistry* **1994**, *33*, 8428.

(2) Zhong, W.; Gulotta, M.; Goss, D. J.; Diem, M. *Biochemistry* **1990**, *29*, 7485.

(3) Gulotta, M.; Goss, D. J.; Diem, M. *Biopolymers* **1989**, *28*, 2047.

(4) Kang, H; Johnson, W. C., Jr. *Biochemistry* **1994**, *33*, 8330.

(5) Kyoguko, Y.; Higuchi, S.; Tsuboi, M. *Spectrochim. Acta* **1967**, *23A*, 969.

(6) Holmén, A.; Broo, A.; Albinsson, B. *J. Phys. Chem.* **1994**, *98*, 4998.

(7) Lord, R. C.; Thomas, Jr., G. J. *Spectrochim. Acta* **1967**, *23A*, 2551.

(8) Savoie, R.; Poirier, D.; Prizant, L.; Beauchamp, A. L. *J. Raman Spectrosc.* **1981**, *11*, 481.

(9) Stepanian, S. G.; Sheina, G. G.; Radchenko, E. D.; Blagoi, Y. P. *J. Mol. Struct.* **1985**, *131*, 333.

(10) Wiórkiewicz-Kuczera, J.; Karplus, M. *J. Am. Chem. Soc.* **1990**, *112*, 5324.

(11) Harada, I.; Lord, R. C. *Spectrochim. Acta* **1970**, *26A*, 2305.

(12) Holmén, A.; Nordén, B.; Albinsson, B. *J. Am. Chem. Soc.* **1997**, *119*, 3114.

(13) Holmén, A.; Broo, A.; Nordén, B.; Albinsson, B. Submitted for publication.

(14) Fucaloro, A. F.; Forster, L. S. *J. Am. Chem. Soc.* **1971**, *93*, 6443.

(15) Fornasiero, D.; Roos, I. A. G.; Rye, K.-A.; Kuruscev, T. *J. Am. Chem. Soc.* **1981**, *103*, 1908.

(16) Matsouka, Y.; Nordén, B. *J. Phys. Chem.* **1982**, *86*, 1378.

(17) Dreyfus, M.; Dodin, G.; Bensaude, O.; Dubois, J. E. *J. Am. Chem. Soc.* **1975**, *97*, 2369.

(18) Gonella, N. C.; Nakanishi, H.; Holtwick, J. B.; Horowitz, D. S.; Kanamori, K.; Leonard, N. J.; Roberts, J. D. *J. Am. Chem. Soc.* **1983**, *105*, 2050.

(19) Chenon, M.-T.; Pugmire, R.; Grant, D. M.; Panzica, R. P.; Townsend, L. B. *J. Am. Chem. Soc.* **1975**, *97*, 4636. Schumacher, M.; Günther, H. J. *J. Am. Chem. Soc.* **1982**, *104*, 4167. Gonella, N. C.; Roberts, J. D. *J. Am. Chem. Soc.* **1982**, *104*, 3162.

(20) Radziszewski, J. G.; Balaji, V.; Cársky, P.; Thulstrup, E. W. *J. Phys. Chem.* **1991**, *95*, 5064.

(21) Radziszewski, J. G.; Downing, J. W.; Gudipati, M. S.; Balaji, V.; Thulstrup, E. W.; Michl, J. *J. Am. Chem. Soc.* **1996**, *118*, 10275.

(22) Arnold, B. R.; Balaji, V.; Downing, J. W.; Radziszewski, J. G.; Fisher, J. J.; Michl, J. *J. Am. Chem. Soc.* **1991**, *113*, 2910.

(23) Becke, A. D. *J. Chem. Phys.* **1993**, *98*, 1372, 5648.

(24) Lee, C.; Yang, W.; Parr, R. G. *Phys. Rev.* **1988**, *B27*, 785.

(25) Stephens, P. J.; Devlin, F. J.; Chabalowski, C. F.; Frisch, M. J. *J. Phys. Chem.* **1994**, *98*, 11624.

(26) Devlin, F. J.; Finley, J. W.; Stephens, P, J.; Frisch, M. J. *J. Phys. Chem.* **1995**, *99*, 16883.

(27) Bakalarski, G.; Grochowski, P.; Kwiatkowski, J. S.; Lesyng, B.; Leszczynski, J. *Chem. Phys.* **1996**, *204*, 301.

(28) Florián, J.; Baumruk, V.; Leszczynski, J. *J. Phys. Chem.* **1996**, *100*, 5578.

(29) Broo, A.; Holmén, A. *Chem. Phys.* **1996**, *211*, 147.

(30) Rauhut, G; Pulay, P. *J. Phys. Chem.* **1995**, *99*, 3093.

(31) El-Azhary, A. A. *Spectrochim. Acta* **1996**, *52A*, 33.

(32) Hedayatullah, M. *J. Heterocyclic Chem.* **1982**, *19*, 249.

(33) Platzek, T *Z. Naturforsch.* **1987**, *42C*, 613.

(34) Denayer, R. *Bull. Soc. Chim. Fr.* **1962**, 1358.

(35) Nordén, B. *Appl. Spectrosc. Rev.* **1978**, *14*, 157.

(36) Michl, J.; Thulstrup, E. W. *Spectroscopy with Polarized Light, Solute Alignment by Photoselection, in Liquid Crystals, Polymers, and Membranes*; VCH Publishers: Deerfield Beach, FL, 1986, (paperback edition, 1995).

(37) Saupe, A. *Mol. Cryst.* **1966**, *1*, 527.

(38) Thulstrup, E. W.; Michl, J.; Eggers, J. H. *J. Phys. Chem.* **1970**, *74*, 3868. Michl, J.; Thulstrup, E. W.; Eggers, J. H. *J. Phys. Chem.* **1970**, *74*, 3878.

(39) Radziszewski, J. G., Michl, J. *J. Am. Chem. Soc.* **1986**, *108*, 3289.

(40) Albinsson, B.; Kubista, M.; Nordén, B.; Thulstrup, E. W. *J. Phys. Chem.* **1989**, *93*, 6646. Albinsson, B.; Nordén, B. *J. Phys. Chem.* **1992**, *96*, 6204.

(41) Albinsson, B.; Nordén, B. *J. Am. Chem. Soc.* **1993**, *115*, 225.

(42) Holmén, A.; Albinsson, B.; Nordén, B. *J. Phys. Chem.* **1994**, *98*, 13460.

(43) Frisch, M. J.; Trucks, G. W.; Schlegel, H. B.; Gill, P. M. W.; Johnson, B. G.; Robb, M. A.; Cheeseman, J. R.; Keith, T.; Petersson, G. A.; Montgomery, J. A.; Raghavachari, K.; Al-Laham, M. A.; Zakrzewski, V. G.; Ortiz, J. V.; Foresman, J. B.; Peng, C. Y.; Ayala, P. Y.; Chen, W.; Wong, M. W.; Andres, J. L.; Replogle, E. S.; Gomperts, R.; Martin, R. L.; Fox, D. J.; Binkley, J. S.; Defrees, D. J.; Baker, J.; Stewart, J. P.; Head-Gordon, M.; Gonzalez, C.; Pople, J. A. *Gaussian 94*, Revision B.3.; Gaussian, Inc.: Pittsburgh, PA, 1995.

(44) Hariaharan, P. C.; Pople, J. A. *Theor. Chim. Acta* **1973**, *28*, 21.

(45) Møller, C.; Plesset, M. S. *Phys. Rev.* **1934**, *46*, 618.

(46) Onsager, L. J. *J. Am. Chem. Soc.* **1936**, *58*, 1486.

(47) Wong, M. W.; Wiberg, K. B.; Frisch, M. J. *J. Am. Chem. Soc.* **1992**, *114*, 1645.

(48) Karelson, M. M.; Zerner, M. C. *J. Phys. Chem.* **1992**, *96*, 8991.

(49) Miertus, S.; Scrocco, E.; Tomasi, J. *Chem. Phys.* **1981**, *55*, 117.

(50) Cossi, M.; Barone, V.; Cammi, R.; Tomasi, J. *Chem. Phys. Lett.* **1996**, *255*, 327.

(51) Coitiño, E. L.; Tomasi, J. *Chem. Phys.* **1996**, *204*, 391.

(52) INTDER95 is a general program developed by Wesley D. Allen and co-workers which performs various vibrational analyses and higher-order nonlinear transformations among force field representations.

(53) Allen, W. D.; Császár, A. G.; *J. Chem. Phys.* **1993**, *98*, 2983.

(54) Allen, W. D.; Császár, A. G.; Horner, D. A. *J. Am. Chem. Soc.* **1992**, *114*, 6834.

(55) Phillips, P. J. *Chem. Rev.* **1990**, *90* (2), 425.

(56) Holmén, A.; Broo, A. *Int. J. Quant. Chem., Quantum Biol. Symp.* **1995**, *22*, 113.

(57) Mcmullan, R. K.; Benci, P.; Craven, B. M. *Acta Crystallogr.* **1980**, *B36*, 1424.

(58) Lin-Vien, D; Colthup, N. B.; Fately, W. G.; Grasseli, J. G. *The Handbook of Infrared and Raman Frequencies of Organic Molecules*; Academic Press: San Diego, 1991; Chapter 2.

(59) Lin-Vien, D; Colthup, N. B.; Fately, W. G.; Grasseli, J. G. *The Handbook of Infrared and Raman Frequencies of Organic Molecules*; Academic Press: San Diego, 1991; Chapter 17.

(60) Hollas, J. M. *Modern Spectroscopy*; Wiley: Chichester, 1992; p 176.

(61) Holmén. A.; Albinsson, B.; Nordén. B. *J. Phys. Chem.* **1994**, *98*, 13460.

(62) To test the predictive capability of the DFT(B3LYP)/6-31G(d,p) method, we used it on propene and the deuterated propenes which have been investigated both experimentally and computationally by Radziszewski *et al.*[21] We obtained transition energies, IR intensities, and polarizations (Table 6S) very similar to their CCSD/6-311(d,p) results.[21] Although far from conclusive, this indicates that the DFT method is useful in order to get rough estimates of IR moment directions.

(63) Holmén, A. Unpublished results.

(64) Foresman, J. B.; Keith, T. A.; Wiberg, K.; Snoonian, J.; Frisch, M.; *J. Phys. Chem.* **1996**, *100*, 16098.

(65) Due to the similarity between the calculated vibrational spectra of both 7-H-adenine and 7MA and between 9-H-adenine and 9MA in the presented frequency region, the calculated frequencies of 7-H-adenine and 9-H-adenine have been scaled with the scaling factors needed to convert the calculated frequencies of 7MA and 9MA to their respective observed frequencies in PVA film. This gave the following scaling factors for the modes corresponding to ν_8, ν_9, and ν_{10} in the methylated derivatives, respectively: 7-H-adenine, 0.987, 0.987 and 0.981 and 9-H-adenine: 0.995, 0.979 and 0.976.